

1-1-2013

# Mechanical And Electro-Chemical Investigation Of Carbon Farbric/epoxy And Aluminum Foam Sandwich Composite Beams

Narin Sara Fatima  
*Wayne State University,*

Follow this and additional works at: [http://digitalcommons.wayne.edu/oa\\_theses](http://digitalcommons.wayne.edu/oa_theses)

 Part of the [Mechanical Engineering Commons](#)

---

## Recommended Citation

Fatima, Narin Sara, "Mechanical And Electro-Chemical Investigation Of Carbon Farbric/epoxy And Aluminum Foam Sandwich Composite Beams" (2013). *Wayne State University Theses*. Paper 230.

This Open Access Thesis is brought to you for free and open access by DigitalCommons@WayneState. It has been accepted for inclusion in Wayne State University Theses by an authorized administrator of DigitalCommons@WayneState.

**MECHANICAL AND ELECTRO-CHEMICAL INVESTIGATION OF CARBON  
FABRIC/EPOXY AND ALUMINUM FOAM SANDWICH COMPOSITE BEAMS**

by

**NARIN SARA FATIMA**

**THESIS**

Submitted to the Graduate School

of Wayne State University,

Detroit, Michigan

in partial fulfillment of the requirements

for the degree of

**MASTER OF SCIENCE**

2013

MAJOR: MECHANICAL ENGINEERING

Approved By:

---

Advisor

Date

## **DEDICATION**

I would like to dedicate this thesis to my father Dr. Md. Jahirul Islam, mother Jesmin Islam, sister Sharin Sara Fatima and my husband Md. Aminul Islam. Without their support and motivation I could have not successfully completed my research work. I would also like to dedicate this to my advisor Dr. Golam Newaz. His guidance and continuous help was one of my biggest motivation throughout the masters program.

## **ACKNOWLEDGEMENTS**

First of all I would like to thank professor Dr. Golam Newaz my thesis advisor for giving me the opportunity to work under him the at the Advance Composite Research Laboratory. His continuous support, guidance and motivation throughout the period of the masters program was my key driving force. I would like to thank Dr. Mohammad Hailat for making me familiar with the experimental lab works. I would also like to thank all my lab partners and friends for their continuous support.

This research was funded by NCMS/DOE (National Center for Manufacturing Sciences/ Department of Energy). I would also like to acknowledge Barrday Advanced Material Solutions for providing the carbon fabric material.

# TABLE OF CONTENTS

Dedication . . . . .	ii
Acknowledgements . . . . .	iii
Nomenclature . . . . .	vii
List of Tables . . . . .	ix
List of Figures . . . . .	x
1 Introduction . . . . .	1
1.1 Sandwich Composite . . . . .	1
1.1.1 Advantage . . . . .	1
1.1.2 Application . . . . .	3
1.1.3 Manufacturing Sandwich Composites . . . . .	4
1.2 Carbon Fabric Skin . . . . .	6
1.2.1 Advantage . . . . .	6
1.2.2 Application . . . . .	7
1.3 Aluminum Foam Core . . . . .	8
1.3.1 Advantage . . . . .	8
1.3.2 Application . . . . .	10
1.3.3 Manufacturing of Aluminum Foam . . . . .	11
1.4 Corrosion in Aluminum . . . . .	16
1.5 Galvanic Corrosion . . . . .	18
1.6 Flexural Test . . . . .	20
1.7 Corrosion Testing (Four Point Probe Method) . . . . .	24
2 Literature Review . . . . .	26
2.1 Introduction . . . . .	26
2.2 Aluminum Foam . . . . .	26
2.3 Aluminum Foam Sandwich Composites Under Flexural Loads . . . . .	27
2.4 Galvanic Corrosion in Sandwich Composites . . . . .	29

3	Objective . . . . .	31
4	Material Design and Sample Preparation . . . . .	32
4.1	Materials Used . . . . .	32
4.1.1	Aluminum Foam Core . . . . .	32
4.1.2	Carbon Fabric/Epoxy Skin . . . . .	33
4.1.3	Glass Fiber/Epoxy Barrier Layer . . . . .	33
4.2	Sample Preparation . . . . .	35
4.2.1	Manufacturing Process . . . . .	35
4.2.2	Trimming and Machining of Composites . . . . .	35
4.3	Corrosion Test Sample Preparation . . . . .	37
4.4	Sample Type . . . . .	39
5	Mechanical Property Testing . . . . .	41
5.1	Flexural Test Experimental Setup . . . . .	41
5.2	Testing Description . . . . .	42
5.3	Failure Modes . . . . .	43
6	Corrosion Testing . . . . .	54
6.1	Four Point Probe Method . . . . .	54
6.2	Experimental Setup . . . . .	55
6.3	Testing Description . . . . .	55
7	Result and Discussion . . . . .	58
7.1	Flexural Test Findings . . . . .	58
7.2	Influence of Barrier Layer on Beams Mechanical Properties . . . . .	60
7.2.1	Damage Location . . . . .	60
7.2.2	Size of Delamination Area . . . . .	61
7.2.3	Permanent Central Deflection . . . . .	61
7.3	Corrosion Test Findings . . . . .	63
8	Comparison Study . . . . .	76
9	Conclusion . . . . .	81

10 Future Work . . . . .	83
Appendix . . . . .	84
References . . . . .	88
Abstract . . . . .	95
Autobiographical Statement . . . . .	96

# NOMENCLATURE

AFS	Aluminum Foam Sandwich
CFRP	Carbon Fiber Reinforced Plastic
CFC	Carbon fabric composite
GFRP	Glass Fiber Reinforced Plastic
E	Young's modulus of elasticity
G	Shear modulus
M	Bending moment
I	Second moment of inertia
1/R	Curvature of plane
b	Width of the beam
t	Thickness of the skin
c	Thickness of the core
d	Thickness of the beam
h	Distance between centerline of upper and lower skin
y	Distance from centroidal axis
$\sigma$	Stress
$\epsilon$	Strain
$\nu$	Poisson's Ratio
L	Span length
P	Concentrated load
$\Delta$	Sandwich beam midspan deflection
D	Beams flexural stiffness
U	Beams shear rigidity
m	Slope of a tangent
Al	Aluminum
e	Electron
H	Hydrogen atom
NaCl	Sodium chloride
V	Voltage
I	Current
R	Resistance
Ca	Calcium
Ti	Titanium



### **Subscript**

f	flexural
core	Beams core
skin	Beams skin
B	Bending
1, 2, 3	Local co-ordinate system

## LIST OF TABLES

4.1	Material properties of Alporas aluminum foam . . . . .	32
4.2	Material properties of EP202 3K 2 × 2 twill carbon fabric. . . . .	33
4.3	Material properties of E-glass/epoxy laminate. . . . .	34
4.4	Physical and geometrical properties of flexural test samples. . . . .	39
4.5	Physical and geometrical properties of aluminum foam core. . . . .	39
5.1	Mechanical properties obtained from the flexural test. . . . .	53
6.1	Sample matrix of sample types and testing conditions. . . . .	56

## LIST OF FIGURES

1.1 Composite sandwich structure. (Source [1]) . . . . .	1
1.2 Comparison between composite sandwich and I beam structure. (Source [2]) . . . . .	2
1.3 Compression molding setup. (Source [3]) . . . . .	5
1.4 Schematic of samples position in mold for autoclave type vacuum press mold. (Source [2])	6
1.5 Different weave pattern schematic: (a) plain, (b) twill, (c) satin. (Source [4]) . . . . .	6
1.6 Aluminum foam. (Source [5]) . . . . .	8
1.7 Various Methods to produce metallic foams. (Source [6]) . . . . .	11
1.8 Direct foaming by gas injection. (Source [6]) . . . . .	12
1.9 Direct foaming using blowing agents. (Source [6]) . . . . .	12
1.10 Powder compact melting method. (Source [6]) . . . . .	13
1.11 Investment casting method. (Source [6]) . . . . .	13
1.12 Electron deposition technique. (Source [6]) . . . . .	15
1.13 Galvanic Cell. (Source [7]) . . . . .	19
1.14 Sample and fixture arrangement for three point flexural test. . . . .	20
1.15 Schematic of a sandwich beam and a cross section through AA. (Source [8]) . . . . .	21
1.16 Experimental setup of the four point probe electrical resistance measurement method. (Source [9]) . . . . .	25
4.1 Alporus aluminum foam used in this study as the sandwich composite core. . . . .	33
4.2 Carbon fabric/epoxy composite material prepreg before curing. . . . .	34
4.3 E-glass/epoxy pre-preg before curing. . . . .	34
4.4 Autoclave type vacuum press machine. . . . .	35
4.5 Cured carbon fabric/epoxy- aluminum foam sandwich panel. . . . .	36
4.6 Flexural test samples prepared from the cured sandwich panel by water jet cutting. . . . .	36

4.7	Flexural test sample geometry and direction from different directions :(a) top view of 250 mm × 25 mm sample, (b) side view 250 mm × 5.8 mm sample, (c) closer view of the sandwich core, (d) auxiliary view. . . . .	37
4.8	Corrosion test sample preparation. . . . .	38
4.9	Closer look at the ends where electrical connections are made. Small hole in the Al foam core to insert copper wires. . . . .	38
4.10	Exposed parts of the sandwich beam sealed using silicon chalk and ends covered by aluminum foil with epoxy layers on top. . . . .	39
5.1	Flexural test fixture placed in MTS machine with computerized data recorder and light setup.	41
5.2	Flexural test specimen setup in the test fixture. . . . .	42
5.3	Typical force versus displacement diagram for type A samples under three point flexural test. . . . .	43
5.4	Sandwich beam undergoing deflection. Moment just before the top skin fails. . . . .	44
5.5	Failure initiated in top skin. . . . .	44
5.6	Crack and delamination in top skin. . . . .	45
5.7	Crack parts of top skin overlapping each other. . . . .	45
5.8	Crack initiating in the core and core crushing continues. . . . .	45
5.9	Core shear with further core crushing. . . . .	46
5.10	Moment just before failure initiates at top skin. . . . .	46
5.11	Top skin fails due to fiber breakage and matrix crack and also leading to slight delamination.	46
5.12	Delamination increasing and core crushing starts. . . . .	47
5.13	Cracked top skin parts overlapping each other. . . . .	47
5.14	Fiber splitting in top skin. . . . .	47
5.15	Core crushing taking place. . . . .	47
5.16	With increased deflection core crushing and top skin delamination increases. . . . .	47
5.17	Typical load versus displacement plot for type B samples. . . . .	48
5.18	Specimen original shape before the flexural test started. . . . .	49
5.19	Failure of GFRP ply of top skin and pore deformation just under the loading pin. . . . .	49

5.20	Failure in the carbon fabric/epoxy plies of top skin and core crushing continuing. . . . .	49
5.21	Core densification and fiber splitting at bottom skin. . . . .	49
5.22	Bottom skin undergoing failure and densification continues. . . . .	50
5.23	Indentation in top skin. . . . .	51
5.24	Top skin failing. . . . .	51
5.25	Core pore deforming laterally and delamination between different plies of top skin increasing. . . . .	51
5.26	Instant width long crack on top skin. . . . .	51
5.27	Delamination at carbon fabric/epoxy and GFRP interface. . . . .	52
5.28	Delamination with increased deflection. . . . .	52
5.29	Example 1 of delamination in type B sample under three point flexural test. . . . .	52
5.30	Example 2 of delamination in type B sample under three point flexural test. . . . .	52
5.31	Typical skin flexural stress versus deflection plot for type A sample. . . . .	53
6.1	Schematic diagram of the four point electrode method used to measure the resistance of the sandwich beams core. . . . .	54
6.2	Experimental set up of the four point probe electrical resistance measurement circuit. . . . .	55
6.3	Samples covered by foams soaked in NaCl solution for corrosion to take place. . . . .	56
6.4	Corrosion test samples with dried salt layer before cleaning. . . . .	57
7.1	Damage location of type A samples. . . . .	60
7.2	Damage location of type B samples. . . . .	60
7.3	Delamination area of type A and type B samples. . . . .	61
7.4	Permanent central deflection of type A samples with standard deviation from the mean value. . . . .	62
7.5	Permanent central deflection of type B samples with standard deviation from the mean value. . . . .	62
7.6	Comparison of permanent central deflection between type A and type B samples. . . . .	63
7.7	Type B unsealed sample after 72 days exposure in room atmosphere. . . . .	64
7.8	Type A unsealed sample after 72 days exposure in room atmosphere. . . . .	64
7.9	Type B unsealed sample after exposure to NaCl solution for 16 days. . . . .	65
7.10	Type A unsealed sample after exposure to NaCl solution for 16 days. . . . .	65
7.11	Typical resistance versus time plot for unsealed type B samples (first type of behavior). . . . .	66

7.12	Unsealed type B sample core after being exposed to NaCl solution for 70 days (first type of behavior). . . . .	67
7.13	Typical resistance versus time plot for unsealed type B samples (second type of behavior).	67
7.14	Unsealed type B sample core after being exposed to NaCl solution for 70 days (second type of behavior). . . . .	68
7.15	Typical resistance versus time plot for sealed type B samples. . . . .	69
7.16	Peeled core of sealed type B sample. . . . .	69
7.17	Peeled core of sealed type B sample with salt patches. . . . .	70
7.18	Typical resistance versus time plot for unsealed type A sample. . . . .	71
7.19	Unsealed type A sample core. . . . .	71
7.20	Typical resistance versus time plot for sealed type A sample. . . . .	72
7.21	Sealed type A sample core. . . . .	72
7.22	Typical resistance versus time plot for unsealed type B samples kept in room environment.	73
7.23	Core of unsealed type B sample kept in room environment. . . . .	73
7.24	Typical resistance versus time curve for type A unsealed samples kept in room environment.	74
7.25	Core of type A unsealed sample after being kept in room environment. . . . .	74
8.1	Unidirectional carbon fiber/epoxy skin and aluminum core sandwich specimen with electrical connections to measure core resistance. . . . .	76
8.2	Exposure to NaCl solution causing delamination between the core and skin. . . . .	77
8.3	Aluminum core sides corroded due to delamination allowing the sandwich samples to be exposed to the NaCl solution. . . . .	77
8.4	Delamination on one side of the core. . . . .	78
8.5	Core corroded in the areas of sample undergoing delamination. . . . .	78
8.6	Skin separated from core due to exposure of NaCl solution. . . . .	78
8.7	Corrosion product on core after removing the skin totally and cleaning the core of above figure. . . . .	79
8.8	Closer look at the corroded core of above figure. . . . .	79

# CHAPTER 1: INTRODUCTION

## 1.1 Sandwich Composite

Sandwich composite structures consist of two skins separated by a core. The skins are generally thin faces of laminates with high stiffness and high strength, and the core is of low density and low stiffness [10]. Just by inserting the core material between the two thin skins the stiffness and strength of a composite structure can be increased to an great extent with adding very little additional weight [11].

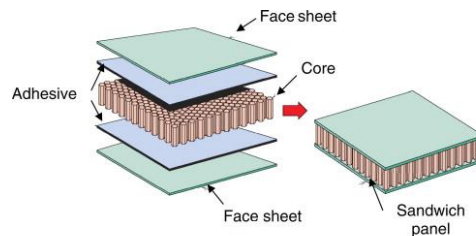


Figure 1.1: Composite sandwich structure. (Source [1])

### 1.1.1 Advantage

High specific flexural stiffness, high strength, shock resistance, acoustic insulation all at a reasonably affordable range can be provided by sandwich composite structures. The main feature of sandwich composite structures is affordability, which is making it become more and more popular for various applications in the aerospace, construction, marine industries [10]. As sandwich composite structure comprises of a low cost core material, sandwich composites are the most preferred structural forms except cases where space limitation is a major factor [12]. Sandwich composite structure follows the design principle of an I-beam. I-beam is very efficient as a structure as most of the material of this structure is carried by the flanges which are located at a distance further most from the neutral axis. The connecting web only contains enough material needed to make a rigid connection between the flanges and to prevent shear and buckling loads. The faces of a sandwich composite represents the flanges and the core represents the connecting web of an I-beam. The bond between the faces and the core must be very strong as the faces

resists the external flexural moment and the core resists the shear loads and also gives support to the faces against buckling. The only difference between the sandwich beams and the I-beams are the faces and core of the sandwich beams comprises of different materials and the core provides continuous support to the faces instead of support in the form of narrow webs [13].

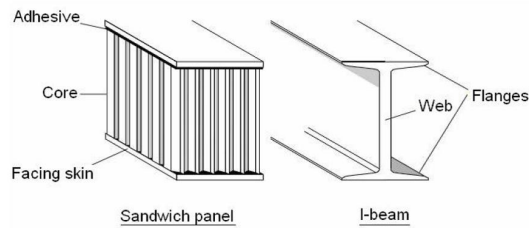


Figure 1.2: Comparison between composite sandwich and I beam structure. (Source [2])

In transportation then main advantage of using composite materials is lightweight, low life cycle cost and crashworthiness. It is seen that some composite designs have better energy absorption capabilities than metal. So during crash a properly designed composite vehicle can dissipate more kinetic energy of the impact than some conventional metals, thus making the vehicle safer. But most of these research have been conducted in the aerospace and motorsports industry where high quality composite materials are used which are out of reach in terms of cost for the mass transportation sector. Due to this, in the transportation industry cost effective composite sandwich structures have become popular as lightweight materials [14].

The sandwich core mainly distributes the shear load. It is able to resist shear and compressive forces better than a single faced laminate structure. They also work as shock absorbers distributing the load between the two skins [11]. Core materials are of very low density in order to add as little as possible weight to the total structure [13]. Compared to the same amount of fiber reinforced polymer materials sandwich composite structures have a higher flexural stiffness [12]. And at the same time improves the flexural rigidity of the structure. So while selecting a core along with its density other properties like shear modulus, shear strength, stiffness etc should also be considered. Sandwich cores are mainly divided in four categories: foams, honeycomb, corrugated and balsa woods [13]. One of the problems with sandwich composite structures is that, there is always a possibility for a weak spot to generate between the skin and the core during loading. For cores like metal foams, honeycomb etc there are lots of pores leading to less solid contact area between the skin and the core. So there is a possibility for the structure to be damaged very easily at the interface [15].



The skin of the sandwich beam is strongly bonded to the core. This is necessary for load transfer between the components. When load is applied on a sandwich beam, one of the skins undergoes compression while the other undergoes tension and the core bears the shear load [2].

Apart from being as light as possible in weight, sandwich composite structures should also have a minimum required stiffness for a certain application, to ensure that it will not fail under the service load. So while designing structures with sandwich composites, the requirements for stiffness and strength and the requirement for minimum weight can be two opposing parameters [16].

### **1.1.2 Application**

Sandwich structures are mostly used because of their lightweight along with high flexural stiffness property. So they are widely used in aviation, ship building and construction where weight saving is critical (Zenkert, 1995, 30).

Lightweight with high strength is making composite sandwich very popular in construction of marine structures [11][8]. These structures provides the vessel with significant weight savings thus reduced fuel consumption and increased payloads and also with built-in thermal insulation and increased stability [11]. These are also being used in making boat transoms and bulkheads [17]. The wind energy industry also uses lightweight sandwich composites for turbine spinners and housings. Sandwich composites are also being used in the wind energy industry due to its reduced transport and installation costs coupled with high levels of noise insulation [11]. Highly loaded sections of the wind turbine rotor blades, spinners and housing are now-a-days mostly made of composite sandwich structures [11, 8, 17]. Another common application of composite sandwich materials are in the aerospace industry. Composite sandwich materials are attracting considerable attention for various load bearing structures of the aircraft fuselages and wing components and also sandwich composite panels are being used in flooring and other interior application of the aircrafts [8, 17]. Sandwich structures are being extensively used in missiles and spacecraft structures due to its high strength to weight ratio [3]. Target applications of sandwich composite materials in the automotive field are for floors, as crash cans, bumpers etc [17]. Composite sandwich are also finding place in sporting goods, civil engineering applications, army tanks, strengthening of structures against earthquake damage [3].

### **1.1.3 Manufacturing Sandwich Composites**

The pre-preg is cut manually to the desired shape to get the plies for the skin. Actual hands-on lay-up process is used to lay up the plies of the skin on top of the core. There are many methods to manufacture composite materials and the most common ones are- vacuum bag processing, autoclave processing, compression molding, filament winding, pultrusion, and braiding. Among these processes to manufacture sandwich composite specimens adhesive bonding, liquid molding, continuous lamination, vacuum bag and autoclave molding are the most common ones.

#### **Adhesive Bonding**

Adhesive bonding is the most simplest of all the processes to manufacture sandwich composite materials. It also has the advantage of providing the sandwich composite with good mechanical properties, well controlled surfaces and most of all this process is independent of the type of the material being used as the core and the skin. Between the skins and the core, adhesive layers are interleaved. Then the whole sandwich composite structure is subjected to increased temperature and pressure depending on the requirements of the adhesive resin and afterwards the cured sandwich is cooled. Generally vacuum bag and autoclave is used for the bonding process [13, 2].

#### **Liquid Molding**

Liquid molding can be done in quite a few different ways such as - Resin Transfer Molding, Structural Reaction Injection Molding and Vacuum-Injection Molding. Liquid molding is very economic and also can produce complex geometrical structures. Among these three different types of liquid molding the resin transfer molding is the most popular one specially in the automotive sector [13]. In this process the uncured sandwich composite specimen is placed in a mold which later with the help of vacuum assistance is infiltrated by resin [2].

#### **Continuous Lamination**

For bulk production continuous lamination method is economical. In this method the skins are guided through the double belt press and the core material is inserted in between them. In this process the sandwich sample can be heated and cooled while at the same time being subjected to certain pressure profile [13].

#### **Compression Molding**

In this process the sandwich composite is placed between two closed dies and the oven temperature

exceeds the melting temperature of the matrix material. The mold closes very quickly and the specimen takes the same shape of the mold. The core material should be carefully selected for this process as it needs to bear the load applied by the closing molds. The main advantage of this process is that, sandwich composite structures with very difficult shapes can be produced and also this process gives very good surface finish of the samples [13].

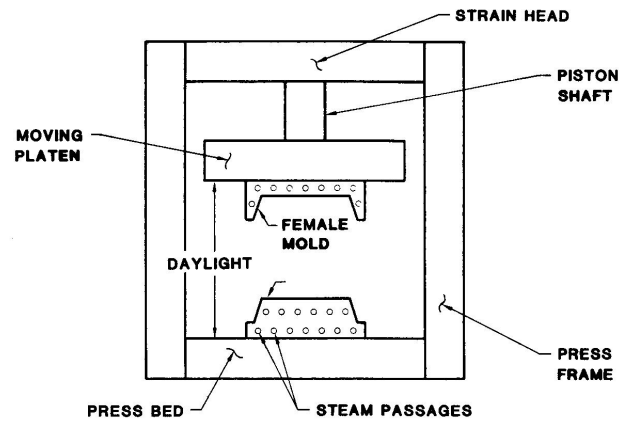


Figure 1.3: Compression molding setup. (Source [3])

### **Autoclave Type Vacuum Press Molding**

In this study to manufacture the sandwich composite specimens an autoclave type vacuum press mold was used. This process was chosen to built the specimens as it gives good mechanical properties with less void content in the samples. After the hand lay up of the pre-preg plies on both side of the core, the samples were placed on the mold of the vacuum chamber, where it under goes the application of sufficient high temperature and pressure for the curing cycle to complete [2]. The sample actually under goes four processes in the vacuum chamber. First the sample is heated respectively in low pressure for a short time then under high pressure where the curing occurs. The samples are cured for 30 minute at 270°F temperature and 50 Psi pressure. After the curing cycle the mist cycle starts which is followed by the cooling cycle.

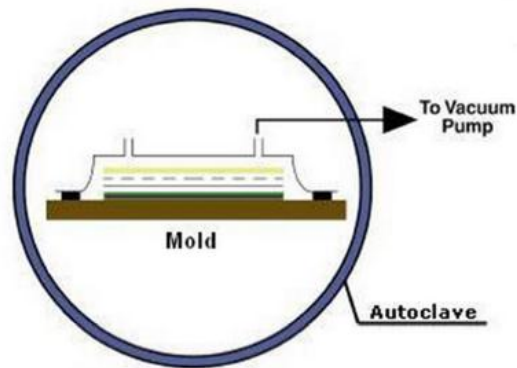


Figure 1.4: Schematic of samples position in mold for autoclave type vacuum press mold. (Source [2])

## 1.2 Carbon Fabric Skin

Woven fabric composite material comprises of an integrally woven two-dimensional fibers impregnated with resin [15]. To get the woven fabric composites first yarns are formed by gathering thousands of fibers. The yarns are then woven in a certain texture to form the woven fabric. Composite fabrics can be of various types depending on the texture, such as plain weave, twill weave, satin weave etc [18].

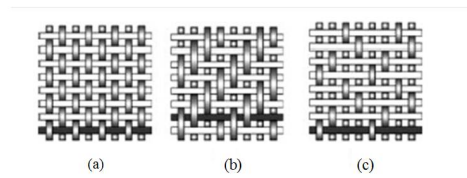


Figure 1.5: Different weave pattern schematic: (a) plain, (b) twill, (c) satin. (Source [4])

### 1.2.1 Advantage

Over the recent years woven fabric composites are becoming more popular over unidirectional tape composites. This is because in woven fabric composites the fiber bundles are interlaced giving better resistance to damaged growth under tension, compression or impact loads. The twill 2/2 woven fabric provides higher specific stiffness, strength and dimensional stability than the unidirectional fiber composite. This is mainly because these fabric composites have balanced bi-directional properties in the fabric plane

[19]. Another advantage of woven fabric composites is that they have the ability to conform to curved surfaces without wrinkling [4].

### **1.2.2 Application**

Woven carbon fabric composites are finding its way into the aircraft industry [4]. Woven fabrics are also being used in marine and sports technology [20].

### 1.3 Aluminum Foam Core

Metal foams like aluminum foam is becoming more and more popular for different applications in the automotive, aerospace, construction industries due to its light weight and good energy absorbing capacity. It represents a combination of unique physical, mechanical, thermal, electrical and acoustic properties [21]. That is why, cellular materials like bone, wood which are similar to metallic foams in structural and functional way are found adequately in the nature. Among the man made cellular foam materials, polymeric foams are most common and widely used [6].

Foam means dispersion of gas bubbles in liquid. And by letting the liquid solidify the morphology of solid foams can be obtained. So solid foams are mainly lightweight structures containing a uniform dispersions of a gaseous phase in a solid. The pores created by the gas are separated from each other by portions of the solid material therefore not allowing the pores to be interconnected [6].

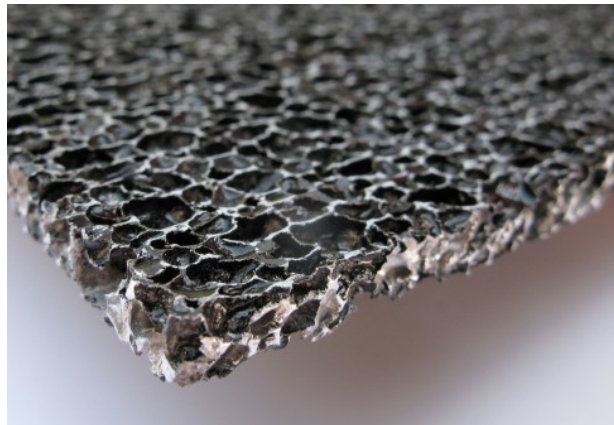


Figure 1.6: Aluminum foam. (Source [5])

#### 1.3.1 Advantage

As metal foams are becoming commercially available now they are largely being used in composite sandwich structures where two stiffened thin outer skins are separated by a central core of metal foam [22]. Aluminum foams have a large rough surface area which provides them good bonding characteristics with the composite skins. The application of these aluminum foam brings in the probability of them being exposed in certain corrosive environments. So it is necessary to investigate the corrosion behavior of these aluminum foams [21].

High Stiffness and strength to weight ratio along with very good impact energy absorption capability offered by the metallic foams are drawing attention in using them as the core material in sandwich composite structures in aero space and auto industry [23, 24]. The combination of these two properties are making possible to design lightweight structures with good crashworthiness properties. Again in compression, flexure and torsion the aluminum foams provide high density compensated mechanical properties [25].

The metallic foams also offer good acoustic damping, thermal insulation, non-combustibility, good electromagnetic wave shielding qualities and low toxicity making it a better alternative to other polymer foams [8, 23]. Closed cell aluminum foams also has excellent toughness [8]. As aluminum foams fail in ductile mode they have a better energy absorption capability [26, 27]. They also have less localized damage [28]. Apart from these other unique properties like high strength and elastic strains, high wear and corrosion resistance, and excellent processability due to low melting temperatures and superplastic-like flow at high temperatures are provided by the metallic foams. These metallic foams mostly in the form of sandwich structures is finding its way in different applications [25].

Polymeric foams such as polyvinyl chloride, polyetherimide and polyurethane are also widely used as core materials in sandwich composite structures. But these polymer based foams suffer from a low heat resistance so in sandwich structures they are used with low temperature curing thermosetting-based composites skins [8]. The mechanical properties of these cores are highly temperature sensitive. So for highly heated thermal environments these systems are not suitable. Due this limitation in curing temperature these foam cores cannot be coupled with some high-temperature curing requiring composite skins which have excellent toughness and a short processing time. On the other hand, lightweight aluminum foams are capable of being cured at high temperature and also to be used in higher temperature applications. So eventually in some applications aluminum foams are replacing the polymeric foams [8].

Using metallic foams as the core in sandwich structures, higher flexural stiffness with minimum increase in weight can be achieved [23]. This is because these metallic foams have very less density but quite significant amount of thickness. Aluminum foams also have low water absorption and low resin uptake leading to weight savings due to reduced resin consumption [11].

Aluminum itself is very impressive in the aerospace and automotive field because of its lightweight characteristic due to its low density. But aluminum foam has even lower density compared to aluminum. Where aluminum has a density of  $2.7 \text{ gm/cm}^3$ , aluminum foam has a density of only  $0.25 \text{ gm/cm}^3$ . Which is nearly 10 times less than the density of aluminum. And by increasing the thickness of the aluminum

foam structures it can achieve the same flexural rigidity of a structure made of aluminum with smaller thickness. Calculation shows that the same flexural rigidity of a 1 mm thick aluminum structure can be achieved by a structure of the same length and width made of aluminum foam just with an increased thickness of 4.64 mm. But the aluminum foam structure will provide the same flexural rigidity at 57% reduced weight. Though aluminum is one of the most lightweight materials available for structures, the use of aluminum foam instead of aluminum can provide more lightweight structures. So as the aluminum foams have sufficient thickness, by adjusting the thickness it can offer the same structural rigidity of an aluminum structure at a lighter density.

Metallic foams have some limitations like poor ductility in the axial direction, pore size control, uniformity of the pores across the structure, isotropy of the foam material etc. And the extent of these limitations depend on the ways the foams are processed. So the properties of these foams can be controlled by controlling the processing parameters. Higher temperature, cooling rate, compositional accuracy, impurity control and difficult processing techniques will give metallic foams with better mechanical properties compared to the base alloys but will also increase the processing cost and steps. So for the metallic foams an inverse relation prevails between better properties and cost effectiveness [25].

### **1.3.2 Application**

Aluminum foams are being used as lightweight structures, impact/blast mitigators, fluid filters, catalytic supports, biomedical implants, sports goods, cellular telephone housings and in many more applications [25].



### 1.3.3 Manufacturing of Aluminum Foam

There are a number of ways to produce metallic foams and some of the procedures are similar to those of producing polymeric foams while some are different. The methods to manufacture metallic foams are classified in four main categories depending on the state the metal is processed in:

1. from liquid metal
2. from solid metal in powdered form
3. from metal vapor or gaseous metallic compounds
4. from a metal ion solution [6]

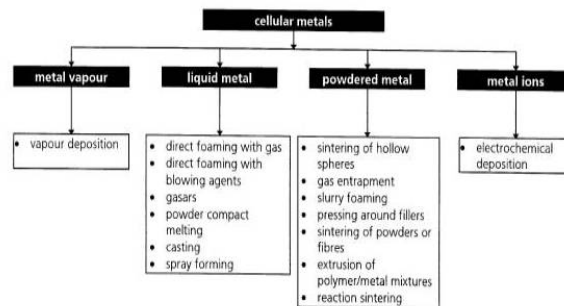


Figure 1.7: Various Methods to produce metallic foams. (Source [6])

#### 1. Liquid State Processing

In this method the metallic foam is processed from molten metal and this can be done in two different ways:

##### Direct Metal Foam:

By creating gas bubbles in molten metal, metallic foams can be created. Due to the high buoyancy forces of the gas bubbles in the high-density liquid metal these bubbles rapidly rises to the liquid surface. The rise of the gas bubbles in the liquid metal can controlled by changing the viscosity of liquid. Direct metal foaming process can be devided in two ways:

- using an external source to inject gas in to the liquid metal
- creating internal gas formation in the liquid metal by adding gas releasing blowing agents

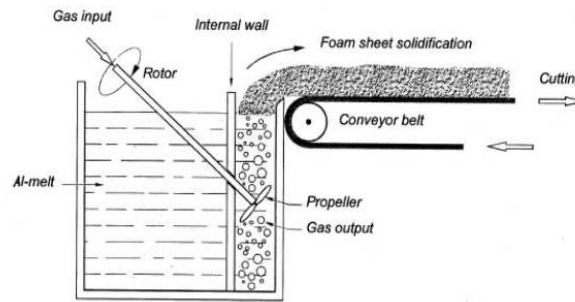


Figure 1.8: Direct foaming by gas injection. (Source [6])

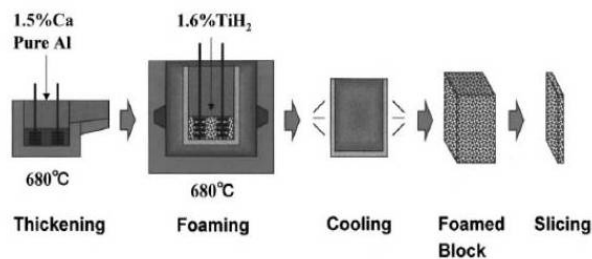


Figure 1.9: Direct foaming using blowing agents. (Source [6])

### Solid-Gas Eutectic Solidification

Some metals when melted in presence of high pressure in a hydrogen atmosphere creates a homogeneous molten metal charged with hydrogen and when the temperature of one of these component is lowered this mixture undergoes an eutectic transition and converts to a heterogeneous two phase mixture of solid and gas. When the temperature of this molten metal is reduced further it leads to solidification. During the solidification process the hydrogen content transforms to gas bubbles. These gas bubbles are not allowed to float out of the liquid metal but by controlling the process parameters are kept entrapped near the solidification zone giving rise to pores after complete solidification of the liquid metal.

### Powder Compact Melting Technique

This method was developed at Germany's Fraunhofer-Institute in Bremen. Though the actual foaming takes place in liquid state this method starts with metal powders so this method is sometimes called the powder metallurgical.

### Casting Methods

Casting method can be of various types, such as:

#### Investment Casting with Polymer Foams

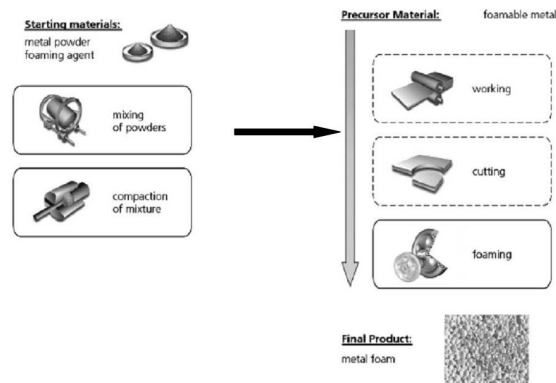


Figure 1.10: Powder compact melting method. (Source [6])

In this process the metal foams replicate the polymeric foams. Depending on the filling of the narrow cavities of the foam by the liquid metal, temperature and pressure can be applied to the mould or it can depend on just gravity. A polymer foam with open cells is used in this process which is filled with a slurry material. The slurry material needs sufficiently heat resistant and mixture of mullite, phenolic resin and calcium carbonate or simple plaster can serve this purpose. After the slurry material is cured by thermal treatment the polymer foam is removed resulting in open voids replicating the polymer foam. Then molten metal is cast into these open voids and metal foam is obtained.

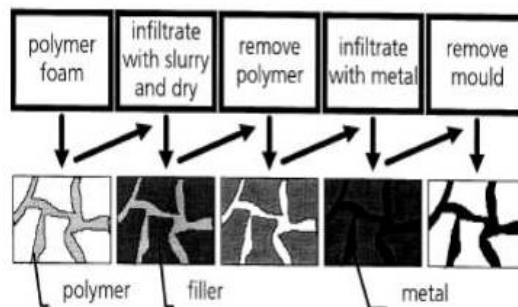


Figure 1.11: Investment casting method. (Source [6])

Other casting methods are lattice block materials casting and casting around space holder material.

### Spray Forming

Molten metal is atomized into small droplets and sprayed on a substrate, where they grow to a dense deposit in a certain shape. To get different properties various powders can be injected in to the spray. This

process provides better quality metal foams than the other casting methods.

## **2. Solid State Processing**

Metal foams are produced from solid metal powders. There are various processes to prepare metal foams using solid metal in powder form, which are given below:

### **Sintering of Metal Powders and Fibers**

This process mainly comprises of preparing the metal powder, compacting it and then sintering it. Sintering increases the density and the strength of the metal foams. Because of the protective oxide layer surrounding aluminum it becomes quite difficult to produce metal foams from metal powder as this oxide layer prevents the metal powders to sinter together. This problem can be solved by adding sintering aids such as copper, silicon, magnesium powders or by deforming the aluminum powder prior to sintering to break the oxide layer.

### **Gas Entrapment Technique**

Metal powders are compressed to a dense precursor material in such a way that gas is allowed to be entrapped in the material. So when the precursor is heated the entrapped gases create an internal pressure leading to expansion of the metal giving rise to the metallic foam.

### **Foaming of Slurries**

Slurry of metal powder mixed with blowing agent and reactive agents is left in a mould at elevated temperature. In the presence of the blowing agent and additives the slurry becomes viscous and expands as gas begins to leave the slurry. This expanded slurry is dried completely and sintered to get the metal foam. This process yields metal foams of high strength. Using this process aluminum foam can be prepared from aluminum powders mixed with orthophosphoric acid and aluminum hydroxide or hydrochloric acid as a blowing agent.

### **Cellular Metals Based on Space Holding Fillers**

In this process ceramic particles, polymer grains, salts, metals etc are used as space holders. The space holding material is filled with fine metal powder and then compacted at room temperature or at elevated temperature. The space holder material is surrounded by a coating of fine metal powders. After compaction the space holding materials are removed by thermal treatment, leaching, or using aqueous solvent. To get better densification the metal foam under goes a sintering process.

### **Metal Powder/Binder Method**

Metallic foams are produced from metal powder and polymer binder mixture. Which are later pressed or extruded to get the foam morphology and then heat treated to get rid of the polymer binder.

### **Reaction Sintering**

In this process multi component metal powder mixture is used and the variation in the diffusion coefficient of these different metals are used to get a porous metallic structure. Example of some of these metal powder mixture is Al + Ti, Al + Fe.

### **Electro-Deposition Technique**

Ionic state of metals in an electrolyte and open cell polymeric foams are used in this process. The metal ions are deposited in the polymeric foam. A thin conductive layer is applied on the foam and after electroplating the foam is removed using thermal treatment.

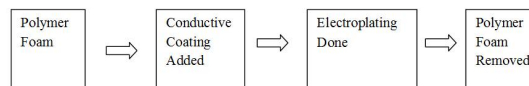


Figure 1.12: Electron deposition technique. (Source [6])

### **Vapor Deposition**

In this process a solid precursor is used which gives the form of the foam. Metal vapor is poured in the cold precursor and allowed to condense. The density of the vapor and the exposure time determines the thickness of the foam. After solidification the precursor is removed by thermal or chemical treatment [6].

## 1.4 Corrosion in Aluminum

Aluminum is a very reactive metal with high affinity to oxygen. But still it has very high resistant against corrosion in most atmospheres and chemical compounds [29]. This is because aluminum spontaneously forms a thin effective oxide layer providing it with a very good corrosion resistance characteristics in most environments [30]. This very thin barrier layer has a thickness between 50 and 100 angstroms. The protective oxide layer is formed around the aluminum surface as soon as it comes in contact with any oxidizing environment such as water, thus completely insulating the aluminum from the surrounding environment [29]. In this way the inert oxide layer prevents any further oxidation to take place on the metal, preventing it from corrosion. This layer actually forms a water proof layer adhering very strongly to the aluminum outer surface and is stable under different environmental conditions. Even if the layer is damaged somehow, it has the ability to instantly repair itself [30].

Most of the time in most environments, for aluminum the rate of corrosion decreases rapidly with time. But in environments containing high concentration of chlorides the case is different and the corrosion rate of aluminum approximately linearly increases with time. So the pH value of the environment strongly effects the stability of the protective oxide film. The oxide film is stable within 4 to 8 pH value. Above and below this range,  $\text{Al}^{3+}$  ions and  $\text{Al}(\text{OH})_4$  ions are formed due to the presence of the acid dissolution and the alkaline dissolution respectively [29].

For galvanic corrosion to take place two conditions must be fulfilled. Both the anodic and cathode material needs to be in contact and an electrolytic bridge must exist between them. Among the two materials the least noble metal works as the anode and the most noble of the materials become the cathode. In a galvanic cell the anode is which under goes corrosion. In sandwich specimen consisting of carbon fabric/epoxy and aluminum foam, the aluminum foam is the least noble metal. So it becomes the anode in the cell and corrodes. When aluminum is in contact with a more noble metal like carbon which can conduct electron with a higher potential than aluminum and at the same time an electrolyte prevails in between them, then this combination will create a galvanic cell [30]. And the aluminum structure will always under go metal loss i.e will be corroded.

Galvanic corrosion does not occur in dry environments in the absence of electrolyte media. So if the dissimilar metals are sealed from the outside environment to prevent it from coming in contact with any type of electrolyte than the possibility of a galvanic cell creation can be stopped. Another way can be by

breaking the electrolyte bridge between the dissimilar metals by painting the metals, coating the cathode, inserting an insulating layer in between them etc. Or the metals can be electrically disconnected from each other by insulating all possible connections. Another way is cathodic protection where with aluminum a less noble material is used as the anode, so that in the galvanic cell the anode will corrode instead of the cathode aluminum [30]. But for the current study, this solution is not possible.

The most common type of corrosion in aluminum is pitting which occurs when aluminum is left in presence of an electrolyte containing dissolved salts. The maximum pit depth is only found to be a fraction of the thickness of aluminum and has no significant effect regarding the strength of the aluminum [30]. The pits will terminate if the pitted surface is remained dry and reactivated again if it comes in to contact with water [29]. Compared to other structural materials even in open air aluminum has better durability. But when aluminum is kept in water specially in stagnant water containing chloride particle it has an adverse effect on the durability of the structure [30].

## 1.5 Galvanic Corrosion

Galvanic corrosion is one of the most common type of corrosion that the real world engineering structures face. It is the corrosion between electrically connected dissimilar metals [31]. This occurs when one metal become predominantly anodic while the other becomes cathodic [32]. When materials with higher electro negative potentials known as cathode are brought in contact with materials with higher electro positive potentials known as the anode and are connected directly or through an external path leads to galvanic corrosion [31]. Electronegativity is a property of an atom to attract electrons towards itself. It depends on the atomic number and distance that its valence electrons reside from the charged nucleus. On the other hand, electropositive materials have a very high tendency to lose electrons from its outer orbit in order to obtain noble gas configuration. According to Pauling scale carbon has a electronegativity of 2.55 and aluminum of 1.61. This potential difference leads them in creating a galvanic cell when brought in contact in presence of an electrolyte.

The main parameters that determine the extent of the galvanic corrosion are- the area ratio of the anode and cathode, conductivity of the electrolyte solution, amount of oxygen present in the solution, the difference between the polarization characteristics of the dissimilar metals, temperature, the efficiency of the cathode etc. But the main driving force to determine the extent of the galvanic reaction is the difference between the potential of the two dissimilar metals that will create the current flow between the anode and cathode of the galvanic cell in the presence of a conductive media [31].

Dry atmosphere does not let a galvanic cell to take place. However, if dissimilar metals are exposed to environments with high levels of chloride such as in the coastal areas they have a high risk for galvanic corrosion [30].

For carbon fabric/epoxy aluminum foam sandwich specimens the carbon fabric skins are very strongly bonded to the aluminum foam core. So for corrosion to occur in these type of sandwich structures, it requires the penetration of water molecules, ions and oxygen through the skins to the interface. It is assumed that even the non damaged samples have small pores or pathways within the epoxy based carbon fiber skins that allows the transportation of the corrosion inducing media in the form of diffusion [33]. Thus leading to corrosion in the samples.

Sandwich composite structures are very prone to damage and can experience various types of defects during its service lifetime from low velocity impact, during maintenance and repair or by any other mean.



These defects may create gaps between the skin and core, rising the probability of direct contact between the corrosive electrolyte and the bare metal. So local defects in the sandwich specimens lead to the most severe corrosion [33].

In presence of an electrolytic solution the anode metal of the galvanic cell under goes oxidation and cathode material experiences reduction which leads to electron transfer between the two electrodes. These two reaction occurs simultaneously and at the same rate. The corrosion of aluminum in water can be represented by the following reactions:-

Anodic reaction  $\text{Al} = \text{Al}^{3+} + 3\text{e}$  Oxidization

Cathodic reaction  $\text{H}^+ + \text{e} = \frac{1}{2} \text{H}_2$  Reduction [29].

As for sandwich specimens with metallic core the corrosion takes place at the skin metal core interface. Therefore, the corrosion depends on a number of parameters such as the state of the sandwich specimen, type of the metallic core, composition of the skin layer, the corrosion products and its transportation mechanism. As corrosion happens at the skin core interface of the sandwich structure and mostly cannot be seen without destructive methods, so to evaluate the progress of corrosion in these cases electrochemical methods are the most suitable tools.[33].

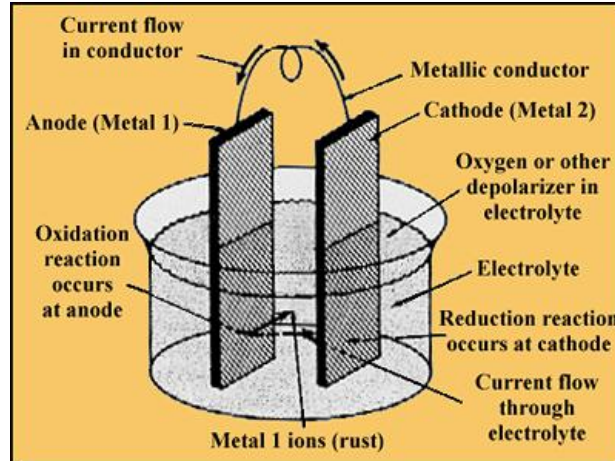


Figure 1.13: Galvanic Cell. (Source [7])

## 1.6 Flexural Test

Sandwich composite beams are mostly appropriate for structures subjected to flexure and impact loads [2]. So in this study a quasi static three-point flexural test was carried out on two different types of sandwich composite structures both consisting of aluminum foam as core. The two different sandwich specimens were aluminum foam with carbon fabric/epoxy skin and aluminum foam core-carbon fabric/epoxy skin with a E-glass/epoxy barrier layer in between them. The purpose of this test was to investigate the structural response of these different sandwich systems under flexural load by analyzing the force-displacement plots and finding the collapse modes, ultimate strength etc.

The tests were conducted according to the ASTM standards C 393 and D 790. These methods are a standard way of finding the sandwich beams flexural strengths and stiffness. The test results are highly sensitive to the sample geometry, span length, loading and support condition [2]. The whole test was recorded by a video from which later digital images were extracted to analyze the different failure modes.

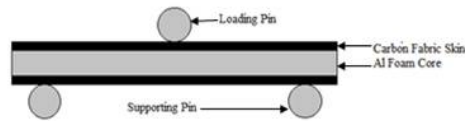


Figure 1.14: Sample and fixture arrangement for three point flexural test.

Under flexural loading sandwich beams can fail by various different mechanisms. The failing mechanism mainly depending on the geometry of the beam and the relative strength of the skins and core [34]. Under compression it is seen that very thin facing laminates act as less effective energy absorbers while thick rigid facing laminates shows a greater probability to fail by localized brittle fracture [14].

Research shows that under high energy impact loading sandwich composites behave in a brittle manner and the skins shows a tendency of de-bonding from the core thus leading to a sudden loss in load-bearing capacity of the structure. Extra reinforcement between the skin and core not only improves the stiffness and strength of the structure, but prevents catastrophic failure originating from skin to core de-bonding [14]. The same behavior is observed for the sandwich composite specimens used in this study under quasi static loading. As long as the skins were the load carrier the sandwich beam behaved in a brittle manner. But with failure of the top skin due to face yielding the load was transferred to the core and from then

ductile behavior of the system was observed.

From the flexural test the following quantities were evaluated: sandwich composites flexural stiffness by interpolating the experimental data in the linear-elastic phase, collapse loads by taking the highest load before the specimens fails and analysing the failure modes from the digital pictures and video clips [24].

### Elastic Flexure of Sandwich Beams

A composite sandwich beam comprises of two thin stiff laminates separated by a thick core of low density and low stiffness. In the flexural test the sandwich beam is subjected to out of plane load. And if sandwich beams are subjected to out-of-plane loading the elastic response can be calculated from formulas established in standard mechanics texts [8]. The following figure shows a simply supported beam subjected to a concentrated load at its center.

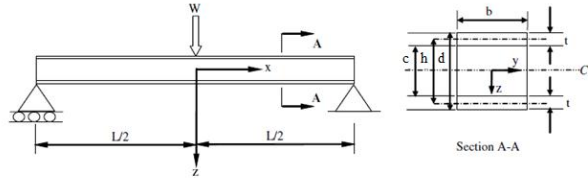


Figure 1.15: Schematic of a sandwich beam and a cross section through AA. (Source [8])

From the engineers theory of flexure we find,  $\frac{M}{EI} = \frac{1}{R}$

where M is the bending moment, E is the Young's modulus of elasticity of the sandwich beam, I is the second moment of area of the cross-section of the beam,  $1/R$  is the curvature of the plane. EI together defines the flexural rigidity of the beam, and for a sandwich composite beam EI is the sum of the separate flexural rigidities of the fiber-reinforced skin and foam core, measured about the centroidal axis of the entire cross-section. So the flexural rigidity of the sandwich beam can be expressed as follows:

$$EI = E_{skin} \frac{bt^3}{6} + E_{skin} \frac{bth^2}{2} + E_{core} \frac{bc^3}{12} \quad (1.1)$$

where  $E_{skin}$  is the modulus of elasticity of the skin,  $E_{core}$  is the modulus of elasticity of the core, b is the width of the sandwich beam, t is the thickness of the skin, c is the thickness of the core, and h is the distance between the centre lines of the upper and lower skins.

$$h = \frac{d+c}{2}$$

The first two terms in equation represent the flexural stiffness of the skins about the centroidal axis of the entire sandwich structure due to flexure. The third term represents the flexural stiffness of the aluminum foam core. Mainly the second term in the equation dominates the response of the sandwich beam. For sandwich beams with thin, high stiffness skins, the first and third terms can be neglected. For this study the carbon fabric skin has a thickness of 0.16 mm and elastic modulus of 44 GPa where as the core has a thickness of 5.2 mm and elastic modulus of 0.7 GPa. Which shows that the skin is very thin but of very high elastic modulus compared to that of the core. So the first and third term in the equation can be neglected.

$$EI \approx E_{skin} \frac{bth^2}{2} \quad (1.2)$$

The longitudinal stress in the skin  $\sigma_{skin}$ , is the product of the skins elastic modulus  $E_{skin}$  and the strain in the skin. During flexure the sections in the structure remain plane and perpendicular to the longitudinal axis, so the strain at distance  $y$  below the centroidal axis is equal to  $My/E$ .

$$\sigma_{skin} = \frac{My}{EI} E_{skin} \quad (1.3)$$

For a simply supported beam the moment at the mid span is  $M = WL/4$ , where  $W$  is the concentrated load. Putting

$$M = \frac{WL}{4} \quad (1.4)$$

and

$$EI \approx E_{skin} \frac{bth^2}{2} \quad (1.5)$$

in the above equation we have,

$$\sigma_{skin} = \frac{WLy}{2bth^2} \quad (1.6)$$

So, the stress in the sandwich skin is re-written as a function of the applied load  $P$ , the support span  $L$ , and the specimen dimensions [10].

According to ASTM standard C 393 for three point flexural test,

Core Shear Stress

$$\tau_{skin} = \frac{W}{(d + c)b} \quad (1.7)$$

Skin flexural Stress

$$\sigma = \frac{WL}{2t(d + c)b} \quad (1.8)$$

Sandwich beam midspan deflection

$$\Delta = \frac{WL^3}{48D} + \frac{WL}{4U} \quad (1.9)$$

where, D = Panel flexural stiffness

$$D = \frac{E(d^3 - c^3)b}{12} \quad (1.10)$$

and U = Panel shear rigidity

$$U = \frac{G(d + c)^2b}{4c} \quad (1.11)$$

From ASTM D 790 flexural stress and flexural strain can be calculated as follow

$$\sigma_f = \frac{3WL}{2bd^2} \quad (1.12)$$

$$\epsilon_f = \frac{3\Delta d}{L^2} \quad (1.13)$$

And modulus of elasticity in flexure,

$$E_f = \frac{mL^3}{4bd^3} \quad (1.14)$$

where m is the slope of the tangent to the initial straight-line portion of the load-deflection curve.

## 1.7 Corrosion Testing (Four Point Probe Method)

Customer demand of high-performance with reduced weight can be offered by the carbon fabric/epoxy aluminum foam sandwich structure but at the same time it requires the understanding of corrosion effects and the protection of the metallic foams from corroding. Therefore, electrochemical methods can be a way for evaluating corrosion at the sandwich interface and can also determine the effectiveness of different protection methods. This approach can promote a better understanding of the corrosion interaction between the skin and the metallic core of sandwich structure without doing any harm to the structure [35].

To monitor the structural integrity of composite materials through damage investigation, several established techniques are available such as acoustic emission, flash thermography etc. But all these techniques utilize the external condition of the samples to dictate its overall condition where as in this technique of monitoring the damage in the core through electrical resistance measurement utilizes the internal properties of the material to detect damage [36].

The electrochemical measurements were performed using the four probe electrode method which is a setup of four electrodes. It measured the resistance of the sandwich core. The concept of this method is that if any corrosion takes place in the specimens then due to the damage of the aluminum foam core the overall resistance of sandwich beam will increase. This increase will indicate corrosion taking place in the sample. Two electrodes of the ammeter and the two electrodes of the voltmeter are connected at the two ends of the sample. A power source is used to induce current through the circuit. The voltmeter reading and the ammeter reading are recorded and the Ohm's law is used to calculate the resistance.

Ohm's Law,  $V = I \cdot R$

Most of the electro chemical methods available cannot provide a fast and cheap technique with easy analytical method for corrosion detection at industrial level [35]. This method of electrical resistance monitoring through four probe electrode is very easy to conduct and at the same time will be much cheaper than any other electrochemical corrosion monitoring methods.

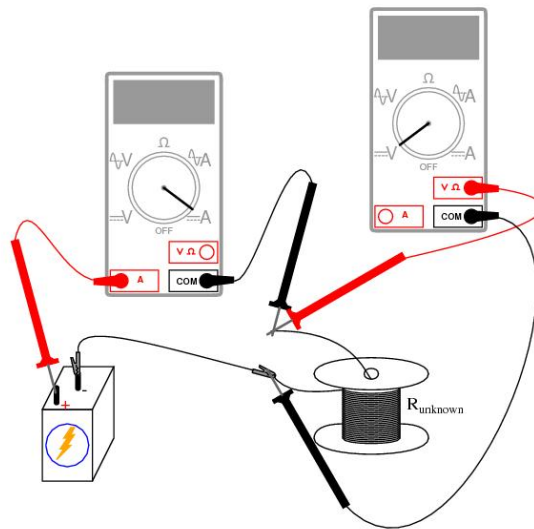


Figure 1.16: Experimental setup of the four point probe electrical resistance measurement method.  
(Source [9])

# CHAPTER 2: LITERATURE REVIEW

## 2.1 Introduction

Composite materials were used by the ancient people since 1500s B.C but modern era of composite materials started in the early 1900s with the development of plastics and fiber glass. Sandwich composites one of the most common structural forms of composite materials have been in use since World War II but the concept was developed much earlier [2]. Many studies have been conducted to understand the behavior of laminated composites subjected to impact, tensile and compressive loads and have been very well documented [12]. Though the concept of sandwich composite is newer compared to laminated composite but many research have also been conducted in this field. Zenkert contributed a lot in understanding composite sandwich beams. Zenkert (1997) in his book documented the fundamentals of sandwich construction along with different theories and failure modes [2].

## 2.2 Aluminum Foam

The concept of metal foam was invented in the early 1900s but the commercial production of it started in the mid 1900s. To determine the mechanical characteristics and failure modes of aluminum foams a large number of studies have been conducted [37, 38, 39, 40, 41]. Evans et al. [38, 39, 42, 43, 44] and Ashby et al.'s [45, 46, 47, 48, 49, 50, 51] series publications report details on the basic characteristic of aluminum foam. Lot of studies have been conducted on experiments of practice aluminum alloy foams [38, 39, 42, 45, 46, 47, 48, 49, 52].



### 2.3 Aluminum Foam Sandwich Composites Under Flexural Loads

Due to its low density aluminum foam became popular as the core of sandwich composite beams. This initiated many study of composite sandwich specimens with aluminum foam as the core under different types of loads such as quasi-static and impact loads. Under quasi static indentation the mechanical behavior of aluminum foam core with different materials such as aluminum, stainless steel, CFRP as skin was investigated. Beams which had adhesive bonding was not only studied but beams with metallic bonds were also studied [37].

Studies showed that the aluminum foam behaves differently under different kinds of loads and different parameters are effected differently with loading condition. For instant for the foam structure the Young's modulus and foam plastic collapse stress are dominated due to flexural load (cell wall flexure), but not for axial load (cell wall stretching) [50, 53]. Again in tension foams deform in a mechanism of cell wall failing ahead of the crack tip and cell edge bridge [47]. For compression, after gradual deformation when cell wall flexure leads to cell crushing and the cells compresses totally from the top and reaches the bottom, then densification starts taking place. So in case of compression densification strain is an important parameter to characterize deformation behavior. After compressive stress drops to the minimum value with start of densification the stress value again starts rising smoothly [43, 44, 46, 50, 52].

The mechanical behavior and experimental results of metallic foams and aluminum foam sandwich (AFS) under static three point flexural load [54, 55, 24, 56] and under four point flexural load [57, 58] have been reported by different researchers. It is seen that under flexural loads, aluminum foam core and aluminum alloy face sheet sandwich composites fail in three modes, which are face yield, indentation and core shear [54, 58]. H. Bart-Smith et al. [53] and C. Chen et al. [58] developed failure maps indicating failure domains of each mode. The failure modes of aluminum alloy faces and foam core sandwich beams can be predicted using these failure maps. The map shows the effect of the geometrical parameters of the beams core and skin on the failure modes by simplified limit load criteria. These maps have been validated against experimental results and finite element analysis of such sandwich beams under flexural fracture and fatigue [52].

The static and dynamic behavior of open cell aluminum foam bonded to two thin skins by acrylate adhesive was studied. The samples had a span length of 250 mm and were loaded in compression and three-point flexural loads and no strain-rate sensitivity was noticed [59]. Aluminum foam sandwich with integral

skins under different loads such as static three-point flexure, buckling and shear tests were also studied [24]. The mechanical responses and failure modes of sandwich and multi layer beams with stainless steel as skin under flexural loading was also studied [52].

Fatigue behavior of sandwich composites consisting aluminum foam core under flexural load was also investigated by many researchers. For these type of sample fatigue crack growth under flexural load has been studied. Also fatigue model of this crack growth have been established and validated [8].

Craig developed a systematic procedure for comparing the relative performance of sandwich beams made from various combinations of materials under three-point flexural loads. The failure mechanisms were described and failure maps were constructed [60]. This study followed some similar study done by Gibson and Ashby and also by Zenkert.

Compared to other studies research with aluminum foam and FRP skin is limited. Aluminum foam as sandwich core provides low density and high impact energy absorption capability. On the other hand, FRP skin comprises of high specific strength and stiffness. Hence, if sandwich beams are made of FRP skins and aluminum foam core than the combined advantage provided by both these materials superpose their individual benefits. So the beams achieve increased flexural stiffness (EI) without a significant weight increase. Studies have been conducted on the response of sandwich beams made of closed-cell aluminum foam core and carbon fiber reinforced epoxy skin under indentation load and the effect of these damage on the residue strength under flexural loading was also studied [61].

## 2.4 Galvanic Corrosion in Sandwich Composites

In early 1700s galvanic corrosion was first recognized when due to corrosion in iron nails holding copper cladding to the wooden hull started falling out and early failure of the ship hull structures were observed [32].

Among the different techniques to assess galvanic corrosion the common ones are measurement of mixed potential, galvanic current, polarization potentials etc. Scanning probe measurement systems such as scanning reference electrode technique (SRET) and scanning vibrating probe technique (SVET) are becoming popular with the advancement in high speed automated data acquisition system, in high resolution scanning mechanism and in microprobe manufacture [32]. Again galvanic corrosion mechanism has been studied by researchers using in situ monitoring of the composite by long focal video microscopy, atomic force microscopy and scanning electron microscopy [62].

By adding epoxy bonding CFRP laminates to the critical stress tensioned area of reinforced concrete or steel structures, their design characteristics can be improved to a great extent. This is an impressive way of repairing structures instead of replacing them as this process takes lesser time and is more cost effective [63]. These type of reinforcement can be added to structures like bridges. But in that case corrosion will be a major factors affecting the serviceability of these structures, especially if it is exposed to cold regions where deicing salts and other aggressive chemicals are available. So there will prevail a very high possibility for galvanic corrosion to take place. If a galvanic cell is created, oxidation will reduce the cross-sectional area of the structure effecting its load carrying capacity. When galvanic corrosion takes place the rate of corrosion also increases thus damaging the structure very rapidly [63].

Mohammadreza Tavakkolizadeh and Hamid Saadatmanesh investigated the possibility of galvanic corrosion between CFRP laminates and steel when bonded together with different epoxy coating at different aggressive environments. The result of this study showed the existence of galvanic corrosion between these combination of material but the corrosion rate can be decreased by applying epoxy coatings. Potentiodynamic polarization and another galvanic test was used in this study where without applying any external potential or current, the current or potential of the two different materials system inside a solution was monitored. To monitor the potential difference between the electrodes a reference electrode was connected to each electrode during the test. The test was continued until a constant current or identical potential between the cathode and the anode was achieved [63].

Fontana 1987 developed the Evans diagram which can be used to estimate the corrosion current density of coupled system. By superimposing the polarization plots of two different materials in one graph such a plot can be obtained. From these diagrams overall corrosion rate of a system can be predicted [63].

Tucker and Brown (1989) investigated the possibility of galvanic corrosion for mild steel coupled with graphite/epoxy and graphite/vinyl ester composites exposed to seawater. After six months of exposure in vinyl ester-based composites noticeable amount of blistering was found. But for the epoxy-based composites no sign of blistering was found. The initiation of these blisters were due to the diffusion of water into the composite and migration of water soluble molecules within the composite [63]. Sloan and Talbot (1992) studied the galvanic corrosion of magnesium coupled with graphite/epoxy composites in seawater. After 140 days of exposure the four point flexural test results showed a 30% decrease in the structures shear strength. They suggested that electrical isolation of carbon fibers and metal by using organic fiber plies and sealer coatings is the simplest way to prevent galvanic corrosion [63]. Cetin (1998) studied the corrosion behavior of reinforced concrete bonded with CFRP and solid graphite rods in seawater. Polarization tests were conducted on the samples. The corrosion rate of graphite rod was found 10 times higher than that of the carbon fibers. Corrosion rate of carbon fibers were lower due to the presence of sizing agents on the surface of fibers [63].

Graphite epoxy composite materials due to its high strength to weight ratio are being widely used in different components of the aircraft structures. These components are connected to other metallic components and under the atmospheric condition this may be a source of galvanic corrosion. F. Bellucci 1992 investigated the effect of the metal to which the graphite epoxy composite materials are coupled with, the effect of temperature, effect of the anode to cathode area ratio and the effect of aging on galvanic corrosion. Results showed large cathode-to-anode area ratio increases the corrosion rate. And also due to ageing the composite losses adhesion. This increases the exposed cathodic area leading to increased corrosion [64].

It is well documented that carbon fiber reinforced plastic when coupled with steel or aluminum induces galvanic corrosion. In 2011 Robert Ireland studied the galvanic corrosion between aluminum 7075 and glass fiber/epoxy composites using some electrochemical methods. This study showed that if the epoxy resin is modified with multi walled carbon nanotubes and kept in an aggressive environment than the corrosion rate and mass loss in these composites becomes double than the composites with the baseline GFRP. In this study the electrochemical measurements of the coupled composite/aluminum samples were conducted using the four-electrode probe method. And this method was found to be quite reliable [64].

## CHAPTER 3: OBJECTIVE

The main objective of this research was to investigate the mechanical and electro chemical properties of a sandwich composite beam made of carbon fabric/epoxy composite laminate as the skin and aluminum foam as the core. The mechanical properties of this system was established through three point flexural test. These sandwich structures may be used in applications exposed to different environmental conditions, some of which may favor corrosion. So it is necessary to monitor the structural condition of these materials using some non destructive methods. Again due to high potential difference when carbon and aluminum brought in contact and an electrolytic media is present, there is the possibility of a galvanic cell formation. Therefore, another main objective of this study was to investigate whether in the presence of an electrolyte, a previously non-conductive composites sandwich structure of carbon fabric/epoxy aluminum foam creates a galvanic cell leading to corrosion. A non-destructive corrosion monitoring technique for these type of sandwich structures can be by measuring the core resistance. This investigation was focused on monitoring the corrosion in the aluminum foam core through the changes in electrical resistance over time in different environmental conditions. And also the effectiveness of different corrosion preventing mechanisms were investigated. So in brief the main objectives of this research are to-

1. Study the mechanical behavior of carbon fabric/epoxy aluminum foam sandwich composite beams under three point flexural load.
2. Investigate the galvanic corrosion behavior of the specimens under different environments and conditions.
3. Monitor corrosion in the beams metal core through a non destructive electrical resistance measurement technique.
4. Study the effectiveness of an glass fiber/epoxy based barrier layer in preventing galvanic corrosion by separating anode from cathode.

# CHAPTER 4: MATERIAL DESIGN AND SAMPLE PREPARATION

## 4.1 Materials Used

### 4.1.1 Aluminum Foam Core

As the core of the sandwich structure Alporas aluminum foam obtained from GLEICH Aluminiumwerk GmbH & Co. KG was used. This aluminum foam is an alloy of aluminum with 1.5% of Ca and 1.5% of Ti. It is a very light weight material with high specific stiffness and has an average density of  $0.25 \text{ gm/cm}^3$ . Throughout, the material consists of pores of 4-6 mm diameter and is considered to have very good homogeneity. These materials are dimensionally stable and at the same time has very good crash energy absorption capability [68]. One of the main advantage of using this material as the core of an sandwich structure is that it has a very rough surface which provides very good bonding with the skin materials. Thus leading to high interface bonding without requiring the use of any additional adhesive. The aluminum foams were provided in  $250 \text{ mm} \times 250 \text{ mm}$  panels with a thickness of  $5 \pm 0.5 \text{ mm}$ .

Table 4.1: Material properties of Alporas aluminum foam

E-modulus (GPa)	0.7
Shear modulus (GPa)	0.3
Shear strength (MPa)	1.2
Ultimate tensile strength (MPa)	1.6
Ultimate compressive strength (MPa)	1.5
Yield strength (MPa)	1.5
Flexural strength (MPa)	2.8
Poisson's ratio	0.33
Coefficient of thermal expansion	$23.4 \times 10^{-6}/\text{K}$

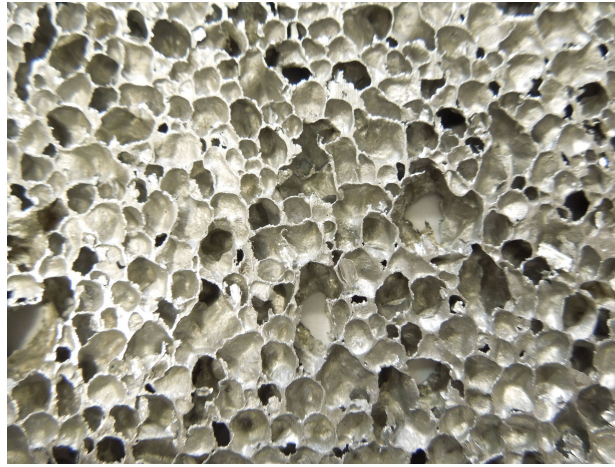


Figure 4.1: Alporus aluminum foam used in this study as the sandwich composite core.

#### 4.1.2 Carbon Fabric/Epoxy Skin

As the skin twill carbon fabric/epoxy pre-pregs named EP202 3K 2 × 2 twill carbon fabric supplied by Barrday Advanced Material Solutions was used. Each skin had two carbon fabric/epoxy plies. Here 3K represents the size of the carbon tow. Carbon tow is a bundle of continuous carbon fibers. The carbon fibers are generally 5-10 microns in size. The tow size is described by the number of the filaments in it. The K indicates multiplication of the filament number by 1000. So a 3K carbon tow contains 3000 carbon filaments in it [65]. EP202 is the epoxy used in the pre-pregs. A speciality of this epoxy is that it does not require post curing. Thus reducing one additional step from the manufacturing process, making the process faster.

Table 4.2: Material properties of EP202 3K 2 × 2 twill carbon fabric.

Tensile Strength (MPa)	689.48
Tensile Modulus (GPa)	43.45
Compressive Strength (MPa)	517.11
Compressive Modulus (GPa)	48.26

#### 4.1.3 Glass Fiber/Epoxy Barrier Layer

As the insulating layer a GFRP ply which was a E-glass/epoxy pre-preg was used. This prepreg was provided by MAG-ias, Cincinnati. It is a cross ply of two 0° and 90° oriented plies stitched together. The

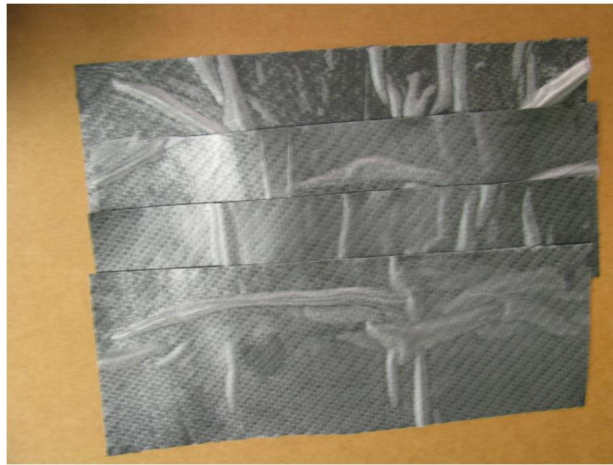


Figure 4.2: Carbon fabric/epoxy composite material prepreg before curing.

resin used is Epon 202 epoxy. All pre-preg rolls were stored in the freezer unless they were cut to make the sandwich beam specimens [2].

Table 4.3: Material properties of E-glass/epoxy laminate.

Tensile modulus, $E_1, E_2, E_3$ , (GPa)	19.8, 19.8, 12.59
Shear modulus, $G_{12}, G_{23}, G_{31}$ , (GPa)	4.04, 3.37, 3.37
Poisson's ratio, $\nu_{12}, \nu_{23}, \nu_{31}$	0.11, 0.18, 0.18
Longitudinal and transverse compressive strength, (GPa)	0.280, 0.280
Longitudinal and transverse tensile strength, (GPa)	0.545, 0.545
Shear strength, (GPa)	0.031



Figure 4.3: E-glass/epoxy pre-preg before curing.



## 4.2 Sample Preparation

### 4.2.1 Manufacturing Process

The plies were hand laid up on the core and no external adhesive was used at the skin core interface. The aluminum foam core was cleaned with a solution of alcohol and water in order to ensure that no grease or any other dirt remained on it. Then the foam cores were dried properly. Two panels of 250 mm  $\times$  250 mm dimension were prepared for the flexural test and two panels of 250 mm  $\times$  75 mm dimension were prepared for the corrosion monitoring test. The autoclave type vacuum press was used to make the samples, where they were cured for 30 minute at 270°F temperature and 50 Psi pressure.



Figure 4.4: Autoclave type vacuum press machine.

### 4.2.2 Trimming and Machining of Composites

The composite sandwich panels made needs to be cut and trimmed to get the samples of the desired size and shape for the mechanical and corrosion tests. Special cutting equipments and operation techniques are required to trim and machine composite materials in a proper way so that it does not lead to any visual splintering or delamination of surfaces or discoloration due to heating [3]. For composite materials with carbon fiber laminate, water jet cutting is the best solution for cutting these materials accurately without damaging the fiber or to avoid any defects (delamination at interface) due to uneven application of force during cutting. So the flexural test and corrosion test samples were prepared from the sandwich panels using water jet cutting. Samples of 250 mm  $\times$  25mm was cut from the 250mm  $\times$  250 mm panels for the

three point flexural test. And from the 250 mm × 75 mm panels samples for the corrosion test was made which were of 75 mm × 25 mm size. The samples were cut using the water jet cutting to get samples of precise size.



Figure 4.5: Cured carbon fabric/epoxy- aluminum foam sandwich panel.

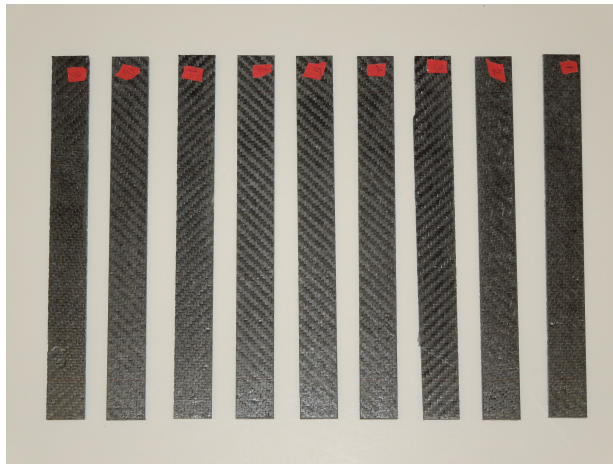


Figure 4.6: Flexural test samples prepared from the cured sandwich panel by water jet cutting.

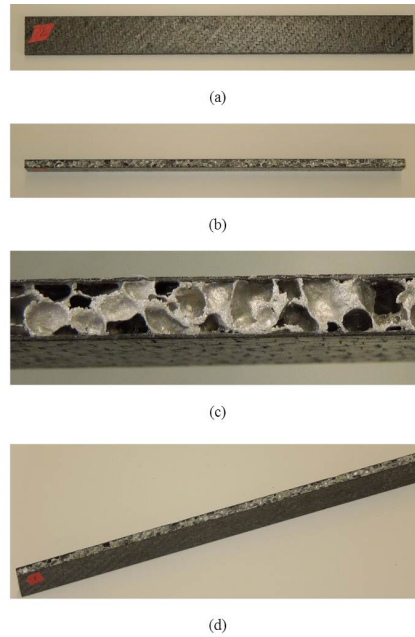


Figure 4.7: Flexural test sample geometry and direction from different directions : (a) top view of 250 mm  $\times$  25 mm sample, (b) side view 250 mm  $\times$  5.8 mm sample, (c) closer view of the sandwich core, (d) auxiliary view.

### 4.3 Corrosion Test Sample Preparation

For the corrosion test sandwich samples of carbon fabric/epoxy-aluminum foam and carbon fabric/epoxy-aluminum foam with the GFRP barrier layer in between having a dimension of 95 mm  $\times$  25 mm were prepared. The samples had a narrower width at both sides where the electrical connections were made. Small holes were made through these smaller cross sectional areas of the foam core along the direction of the samples width. Copper wires were inserted through the holes and secure connections were made. The other ends of the wires were connected to a small crocodile clip to make easy connection with the other apparatus of the circuit. The exposed parts of the wires were wrapped with aluminum foil paper and a thick layer of epoxy was applied on top of it, to prevent any type of interaction with the environment. The Al foils were used to avoid directly supplying the epoxy on the copper wire, as this may effect the electrical conductivity of the wires.

The electrical connections were made only through the cores as the resistance of the carbon fabric/epoxy composite laminates are several times higher than that of the aluminum foam core. The skin acts

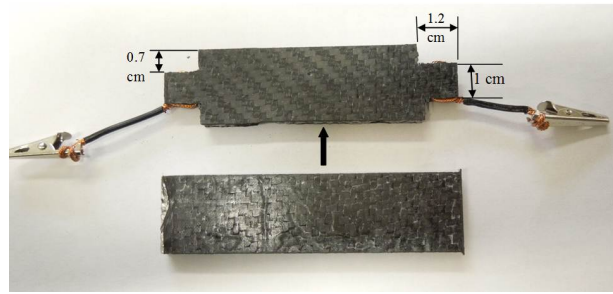


Figure 4.8: Corrosion test sample preparation.

as nearly nonconductive material. So if the resistance of the total sandwich sample is measured through the sample thickness than due to this high resistance of skin the change in the resistance of the aluminum foam might not be noticeable. Therefore, it was decided to measure the resistance change of the aluminum foam core only instead of the entire sandwich beam.

Silicon chalk was used as the sealing material and layer of epoxy was applied on top of it. The purpose of using this sealing was to make the sandwich composite totally sealed from the surrounding environment, so that if any change in electrical resistance takes place that will be totally due to the creation of a galvanic cell.

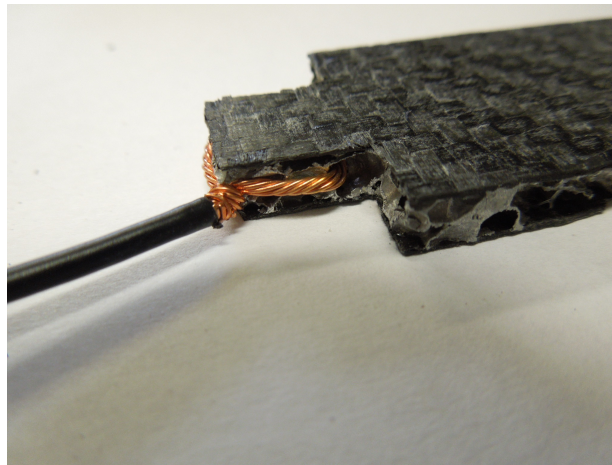


Figure 4.9: Closer look at the ends where electrical connections are made. Small hole in the Al foam core to insert copper wires.



Figure 4.10: Exposed parts of the sandwich beam sealed using silicon chalk and ends covered by aluminum foil with epoxy layers on top.

#### 4.4 Sample Type

The samples for the flexural test and the corrosion test were of two type. Type A samples had two plies of the carbon fabric/epoxy composite on both side of the aluminum foam. And type B samples had a layer of E-glass/epoxy composite in between the carbon fabric/epoxy skin and the aluminum foam core. Due to the difference in the presence of the GFRP ply, type A and type B samples had different thickness and density.

Before undergoing the test procedure, the sample were accurately weighed and their geometrical dimensions were measured using a slide caliper. For type A and type B flexural test samples the mean values and standard deviations of the measures parameters have been reported in the table below.

Table 4.4: Physical and geometrical properties of flexural test samples.

Flexural Test Sample Type	Length (mm)	Width (mm)	Thickness (mm)	Weight (gm)	Density (gm/cm <sup>3</sup> )
A	250	25.22 ± 0.31	5.81 ± 0.05	19.44 ± 0.37	0.53 ± 0.01
B	249.1 ± 0.3	25.30 ± 0.15	6.42 ± 0.07	30.02 ± 0.63	0.74 ± 0.02

The density weight and thickness of the flexural test samples cores are given in the below table.

Table 4.5: Physical and geometrical properties of aluminum foam core.

Thickness (mm)	Density (gm/cm <sup>3</sup> )
5.2	0.25

For type A flexural samples the total average density was  $0.53 \text{ g/cm}^3$  and for type B flexural samples it was  $0.74 \text{ g/cm}^3$ . The average core density was given by the manufacturer as  $0.25 \text{ g/cm}^3$ . The only difference between the samples for the flexural test and the corrosion test was the length of the samples. The flexural test samples had a length of 250 mm where as those for the corrosion test had a length of only 75 mm.

# CHAPTER 5: MECHANICAL PROPERTY TESTING

## 5.1 Flexural Test Experimental Setup

The samples were made according to the ASTM standards provided for the flexural test. ASTM C393 provides the standards for flexural properties of sandwich structures [66]. According to the standard the samples were prepared of rectangular cross section with recommended length and width [22].

Apart from the sample geometry the test set up and the testing process was also done according to the standards. The three point flexural test was conducted at room temperature using the MTS electromechanical compression testing machine having a load capacity of 200 KN. The test was conducted using a fixture provided by Wyoming Test Fixtures Inc. The fixture was of two parts, the loading pin and bottom support. The head of the loading device and the two supports pins were all small steel cylinders. The loading pin had a diameter of 12.7 mm and was securely fixed to the upper cross head of the machine. The bottom support had two pins of the same diameter and was placed on the machine in such a way that the loading pin was exactly over the mid-span of the beam. The two pins of the lower fixture was adjusted to get the desired span length. The midpoint movement imposed by the loading pin directly on the samples was 0.05 mm/sec.



Figure 5.1: Flexural test fixture placed in MTS machine with computerized data recorder and light setup.

## 5.2 Testing Description

The tests were done in displacement control mode where the bottom support moved in an upward direction resulting in the loading pin to push against the sandwich composite beam at a strain rate of 0.05 mm/sec. A load transducer situated on the cross head of the machine records the load taken by the beam to deflect. For every 0.05 sec load and the corresponding displacement data were recorded by the computerized controlled machine.

According to the ASTM test procedure the span length should be kept 16 times more than the total laminate thickness. In this experiment the test samples had a total length of 250 mm and the thickness of the samples were  $5.81 \pm 0.05$  mm and  $6.42 \pm 0.07$  mm respectively for type A and type B samples. So a length of 200 mm was kept as the span length which is more than 16 times the laminate thickness and allowing a length of 25 mm on both edges of the samples to remain as the overhang. Higher span length was kept as it allows greater moments without exceeding the allowable limit for core shear stress [2].

From the recorded load and displacement data the load versus displacement plots were generated to analyze the test results. The whole test process was captured by video. Later which was correlated with the load versus displacement plots depending on time.

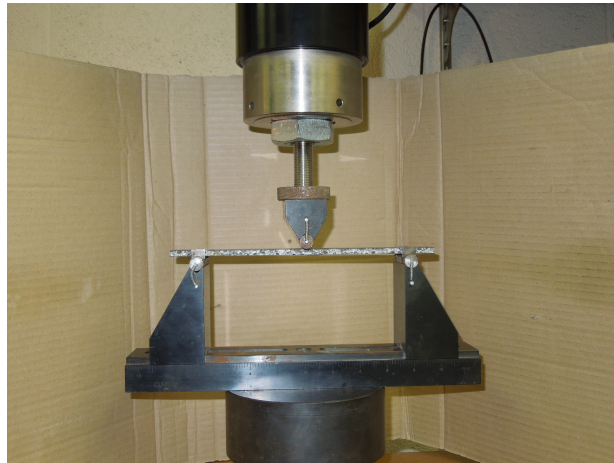


Figure 5.2: Flexural test specimen setup in the test fixture.



### 5.3 Failure Modes

Typical force versus time curves and corresponding photographs of the flexural test of sandwich specimens were compared and it was found that both type of the specimens failed under different failure modes which discussed below.

#### Type A Samples

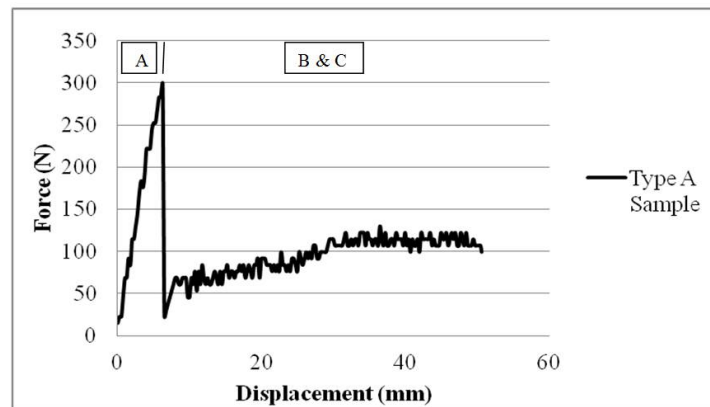


Figure 5.3: Typical force versus displacement diagram for type A samples under three point flexural test.

Zone A: Load carried by the top skin (figure 5.3)

Zone B: Large drop in load due to failure of the top skin and load transferred to the core (figure 5.3)

Zone C: Densification taking place (figure 5.3)

For type A samples under the three point flexural test the force-displacement plots obtained can be roughly divided into three regions. All the samples of this category shows nearly the same behavior in the first two regions but tend to differ from each other in the final phase. Some samples under goes core shear while others do not.

1. From the load displacement curve of all the samples, initially a linear region of deformation is found where the load carrying capacity of the samples increases with deformation. This corresponds to indentation of the loading pin in the composite beams top skin. This deformation represents linear elastic deformation of the beam [22]. At this stage if the load is stopped being applied and the top loading pin is removed from contact of the sample composite beam, then it is seen that the specimen returns to its original position.

2. With an further increase in load, the load-deformation plot deviates from its linearity, leading to a sudden large drop in load. This sudden drop in load is assisted by damage in the top skin. Fiber breakage and matrix crack initiates and with increase in load this damage keeps propagating along the width of the composite beam. This behavior is also noticed for all the samples.
3. As the flexural test proceeds with further displacement the top skin near the area of damage starts initiating delamination.
4. As the load is transferred from the top skin to the core, densification of the core area under the loading pin starts taking place. The sharp drop in the load displacement curve stops at a much lower load value as the load is transferred from the top skin to the core. And due to this densification of the core from this lower level of load with further increase in displacement the load slightly increases. All the samples show the same nature up to this stage.

For some samples with large displacement the bottom skin undergoes localized tension due to the top loading pin [22]. This leads in a creation of slight delamination between the core and the bottom skin and fiber breakage takes place. For some samples the second region showed a decrease in load with increase in displacement. This is due to initiation of crack in the core leading to core shear.

#### **Behavior of Type A Sample with a Core Shear:**

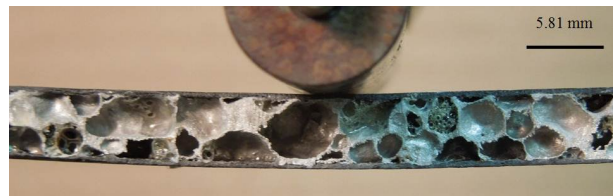


Figure 5.4: Sandwich beam undergoing deflection. Moment just before the top skin fails.



Figure 5.5: Failure initiated in top skin.

Suddenly width long crack develops in top skin. Leading to sudden drop in load.

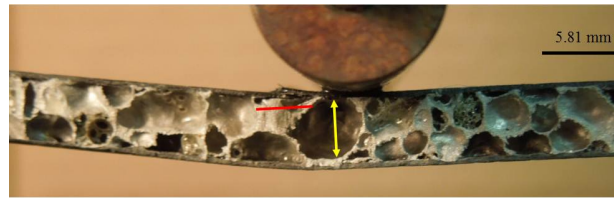


Figure 5.6: Crack and delamination in top skin.

The crack in the top skin does not lead to much of a delamination. With further displacement the cracked delaminated face parts start to overlap each other and during this phase the core is the main load bearing component. Throughout the test strong bond exists between the core and the lower skin.

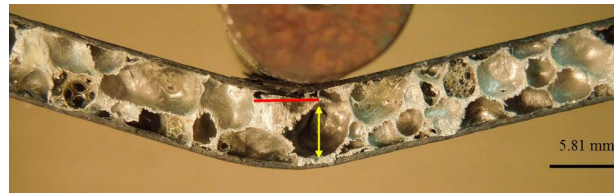


Figure 5.7: Crack parts of top skin overlapping each other.

Cracked de-bonded skin parts overlaps each other and loading pin gradually moves on top of it as the flexural displacement increases. Also core crushing takes place. The yellow arrow in the pictures are indicating the collapse of a certain pore in the core. Comparing the previous picture and this one, it can be seen that due to displacement the diameter of the pore is decreasing. And the red line is indicating the delamination size. It can be seen from these three pictures that with increase in displacement the delamination size has not increased much. Only the crack portion of the top skin are overlapping each other. Due to strong interface bond prevailing between the skins and core, the delamination area did not increase much.

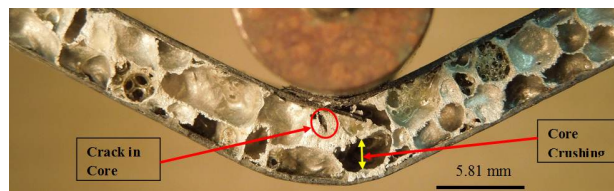


Figure 5.8: Crack initiating in the core and core crushing continues.

Small crack initiates in the core and with further flexural displacement the crack propagates leading to core shear. Slight wrinkle of the damaged top skin was observed. Core crushing continuous taking place.



Figure 5.9: Core shear with further core crushing.

So by noticing the length change of the yellow line over the pore in the core situated under the loading pin the core crushing can be clearly seen. This core crushing leads to densification so the load bearing capacity of the sample increases.

#### **Behavior of Type A Sample without Core Shear:**

Initially the sandwich beam under goes flexural deflection without any damage in the samples.



Figure 5.10: Moment just before failure initiates at top skin.

The top skin in this phase is taking all the load. This is a moment just before the top skin fails so this indicates the moment when the load is maximum at the end of the linear elastic region of the load-deflection plot.

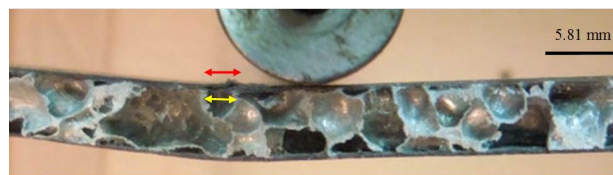


Figure 5.11: Top skin fails due to fiber breakage and matrix crack and also leading to slight delamination.

The top skin fails with a sudden drastic drop in the load of the load-displacement curve.

As the top skin fails the load is transferred to the core. The core carries load in the form of core crush. Comparing the length of a pore of this picture with the previous picture, crushing of the pore in lateral direction can be observed.

With further displacement the fractured sides of the top skin start overlapping each other.

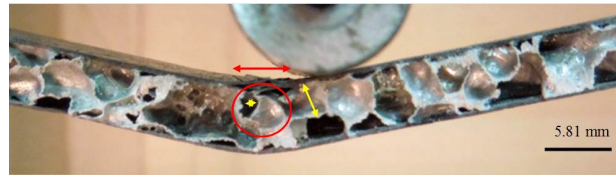


Figure 5.12: Delamination increasing and core crushing starts.



Figure 5.13: Cracked top skin parts overlapping each other.



Figure 5.14: Fiber splitting in top skin.

Fiber splitting occurs at the damaged top skin parts.

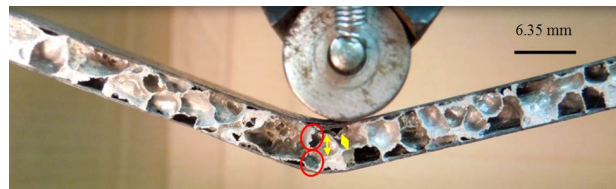


Figure 5.15: Core crushing taking place.

The yellow arrow and red circles showing various pores under the loading pin undergoing crushing.



Figure 5.16: With increased deflection core crushing and top skin delamination increases.

Core crushing leads to densification. And at the same time due to increased bending the length of the

delaminated area on the left side of the loading pin increased. The red arrow is showing the growth of the de-bonded area of the top skin and the core. During the entire test procedure with increased flexural displacement the delamination size did not increase much from that initially originated from the failure of the top skin. But at the end of the process with severe core crushing, the delaminated area suddenly increased a little. From the yellow arrows at different locations of the core it can be seen that, due to densification the foam pore shape has reduced and changed both in the vertical direction and also in lateral direction.

For this sample core shear has not taken place. The core is only crushing due to the flexural displacement leading to densification. This is why the third portion of the force-displacement plot is going up.

### Type B Samples

All type B samples follow the same behavior under the flexural test. The force versus displacement plot for these type of samples can be divided mainly in three regions. Load carried by the top skin, failure of the top skin and transfer of load to the core, densification of the core, these are the main three mechanisms type B sandwich beams undergoes in the flexural test.

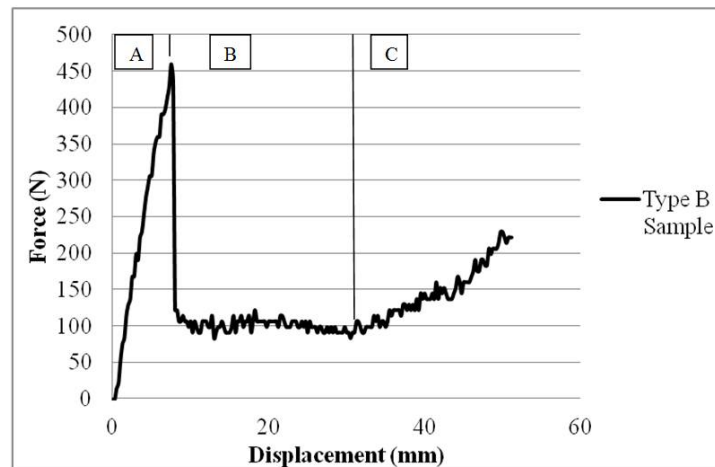


Figure 5.17: Typical load versus displacement plot for type B samples.

Zone A: Increase in load with increased displacement. Load carried by the top skin.

Zone B: Sudden drop in load followed by a plateau stress region. Failure of the top skin leads to transfer of load to the core.

Zone C: Gradual increase in load. Densification of the core increases the load bearing capacity of the

sandwich beam.

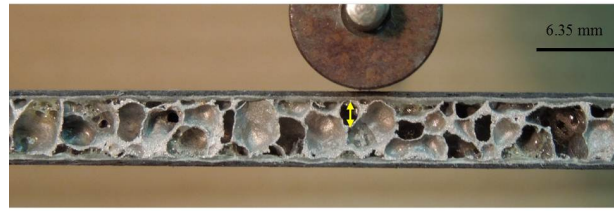


Figure 5.18: Specimen original shape before the flexural test started.

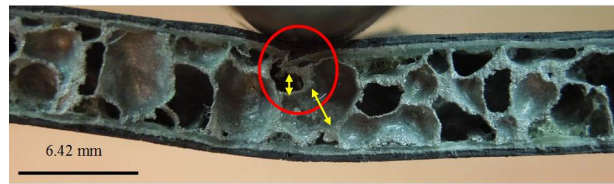


Figure 5.19: Failure of GFRP ply of top skin and pore deformation just under the loading pin.

As the flexural process progresses the GFRP layer of top skin fails while the carbon fabric plies does not experience any fiber breakage or matrix cracking at that moment. But slight delamination between the two plies take place. From the yellow arrow it can be seen that the pore in the core just under the point where the failure in the GFRP occurs, has started undergoing deformation.



Figure 5.20: Failure in the carbon fabric/epoxy plies of top skin and core crushing continuing.

Carbon fabric plies starts to undergo fiber breakage and matrix crack at this stage. The yellow circle shows the core crushing still progressing and the pore walls nearly touching each other.



Figure 5.21: Core densification and fiber splitting at bottom skin.

Different pores deforms and densification in the area marked by the yellow circle taking place. Fiber splitting started at the bottom skin. It can be seen that for the failure of the top skin, slight de-bonding between the plies has taken place which is only between the carbon fabric and GFRP plies. The carbon fiber/epoxy ply is still strongly bonded to the core.

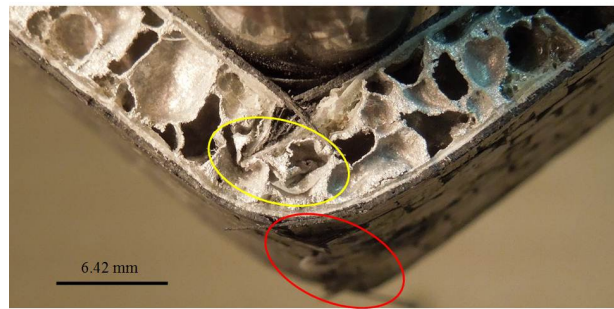


Figure 5.22: Bottom skin undergoing failure and densification continues.

The damage in the bottom skin increasing along the width of the sample and more core crushing and densification taking place. GFRP layer breaks first while the carbon fabric layers only experience indentation. With further displacement the carbon fabric plies break. Core crushing takes place leading to damage of the bottom skin. For the bottom skin only the carbon fabric plies under goes fiber breakage. The GFRP ply remains intact.

The cases where delamination takes place it is seen that the delamination mainly takes place between the GFRP and the core and the GFRP and the carbon fabric layer. For the delamination between the GFRP and the carbon fabric plies, initially between the two plies of the carbon fabric the top one experiences fiber breakage and matrix crack. Which with further displacement becomes a weak spot for delamination initiation. Delamination initiates from this location but propagate at the interface between the carbon fabric plies and the GFRP ply. In most case the delamination between the carbon fabric plies and GFRP ply is greater than that between the GFRP and core.

The following figures shows the failure modes in another type B sample.

Indentation takes place under the loading pin. As the Al foam core does not have a smooth surface the indentation cannot be clearly seen. This is the maximum indentation before the top skin experiences damage.

The top skin under goes failure. The location of the damage area for the carbon fabric plies and the GFRP ply occurs at different places.





Figure 5.23: Indentation in top skin.



Figure 5.24: Top skin failing.



Figure 5.25: Core pore deforming laterally and delamination between different plies of top skin increasing.

Delamination between the carbon fabric plies and the GFRP ply takes place and also core crushing occurs. The loading pin slowly moves towards the fractured parts of the carbon fabric top skin.

Studying the failure modes in some other samples it can be seen from this picture that the crack in the top skin occurs along the whole width of the sample instantly.



Figure 5.26: Instant width long crack on top skin.

Maximum delamination occurs at the interface of the different plies. Not much at the GFRP core interface

As the flexural displacement increases the delamination between the different plies increases.



Figure 5.27: Delamination at carbon fabric/epoxy and GFRP interface.



Figure 5.28: Delamination with increased deflection.

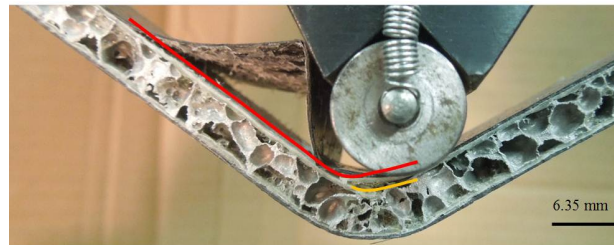


Figure 5.29: Example 1 of delamination in type B sample under three point flexural test.

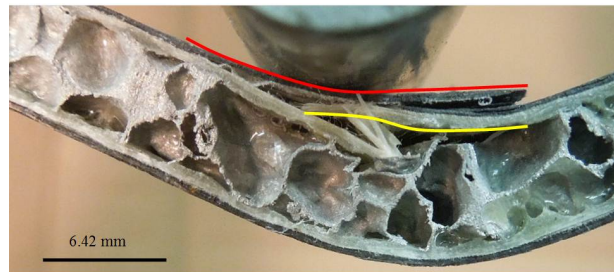


Figure 5.30: Example 2 of delamination in type B sample under three point flexural test.

The red line is representing the length of the delamination at the interface of the carbon fabric plies and the GFRP ply of the top skin. And the yellow line representing the delamination length at the interface of the top skin and the core i.e. between the GFRP ply and the core. It is again seen that for each case the delamination between the different material plies of the top skin is greater than that between the GFRP ply and the core.

The skin flexural stress was calculated according to ASTM C 393 and also according to the beam

Table 5.1: Mechanical properties obtained from the flexural test.

Sample Type	Maximum Force (N)	Ultimate Displacement (mm)
A	$333.9 \pm 15.1$	$6.95 \pm 0.44$
B	$500.0 \pm 36.8$	$7.42 \pm 0.71$

elastic theory and plotted against deflection. By comparing both the curves it was seen that both results give nearly the same amount of stress value.

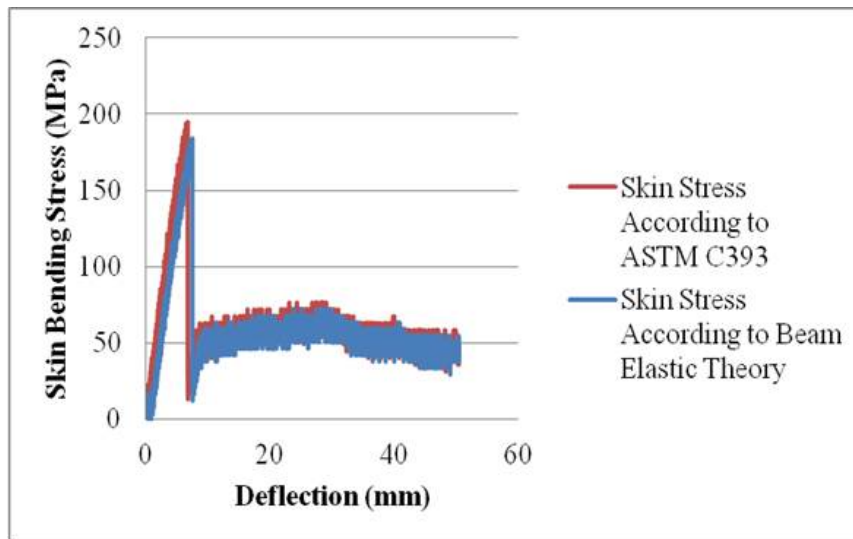


Figure 5.31: Typical skin flexural stress versus deflection plot for type A sample.

Using the formulas provided in ASTM D 790 the flexural stress and flexural strain were calculated [67]. From which the modulus of elasticity in flexure  $E_f$  was calculated. For the type A samples the value of  $E$  was found to be 35.41 GPa.

## CHAPTER 6: CORROSION TESTING

### 6.1 Four Point Probe Method

The main objective of this study was to investigate whether in the presence of any electrolyte the carbon fabric/epoxy-aluminum foam sandwich composite material creates a galvanic cell. Four point probe electrical resistance measurement method was used to monitor corrosion of the sample cores through change in electrical resistance. The four point probe electrical resistance measurement method is also known as the Kelvin 4-wire resistance measurement. The main reason for using this circuit is because it reduces contact resistance [68]. In this method the change in ohmic resistance of a metallic specimen exposed to an aggressive corrosion inducing environment is measured. Corrosion of a metal leads to decrease in its cross-sectional area resulting in an increase in its electrical resistance [69]. In this method four electrodes are connected to the sample for measuring resistance. Two electrodes supply the current to the sample while the other two measures the voltage over the sample due to this current flow. A schematic diagram of the arrangement is shown below:

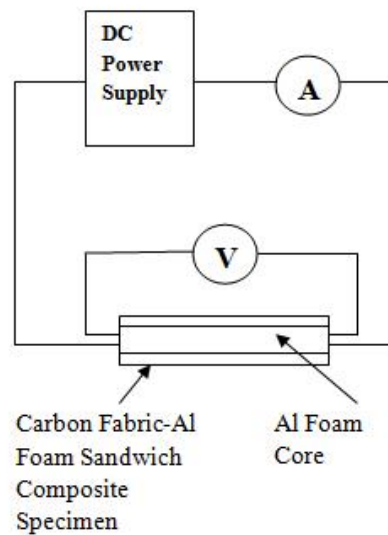


Figure 6.1: Schematic diagram of the four point electrode method used to measure the resistance of the sandwich beams core.

## 6.2 Experimental Setup

In this study to establish the four probe electrode circuit the current was induced using a DC power supply and two tektronix multimeters were used, one acting as the ammeter and another as the voltmeter.

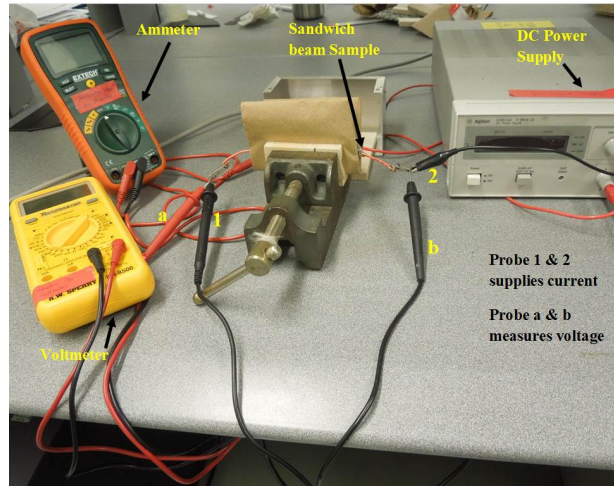


Figure 6.2: Experimental set up of the four point probe electrical resistance measurement circuit.

## 6.3 Testing Description

The electrical resistance measurement samples were of several types. And the measurements were carried out at two different environmental conditions, one at ambient atmosphere and the other using chloride containing aqueous electrolyte solution. The sample matrix below shows the sample types and the testing conditions.

3.5 wt% NaCl water solution was used as the corrosion inducing media. The reason behind selecting this concentration of NaCl was to represent conditions in natural coastal atmospheres and on surfaces that are in contact with de-icing salts [70].

Initially the samples were kept in ambient condition to monitor whether the presence of normal room humidity leads to any change in the electrical resistance of the core i.e. whether in room environment any corrosion is taking place in the specimens.

Then the samples were covered from both side by small pieces of foams soaked in 3.5% NaCl solution. The reason behind covering the samples by foams soaked in 3.5% NaCl instead of immersing the samples

Table 6.1: Sample matrix of sample types and testing conditions.

Sample Type	Environmental Condition	Sample no.
CFC - Al foam Sandwich Composite Samples	Kept in aggressive environment	3
CFC - Al foam Sandwich Composite Samples with the sides covered with insulating layer	Kept in aggressive environment	2
CFC - GFRP - Al foam Sandwich Composite Samples	Kept in aggressive environment	3
CFC - GFRP - Al foam Sandwich Composite Samples with the sides covered with insulating layer	Kept in aggressive environment	2
CFC - Al foam Sandwich Composite Samples	Kept in normal room environment	2
CFC - GFRP - Al foam Sandwich Composite Samples	Kept in normal room environment	2



Figure 6.3: Samples covered by foams soaked in NaCl solution for corrosion to take place.

in NaCl solution is that, for applications of the carbon fabric aluminum foam sandwich beams other than in marine sector, the samples will not always be immersed in an electrolyte. Instead sometimes during its service life it might come in to contact with the electrolyte. For example if an external part of an automobile is made of such composite sandwich and while driving in the roads a splash of de-iced water falls over it. Eventually the electrolyte will dry up. The external automotive sandwich composite parts might come in contact with the electrolyte solution several times during its service life. In that case, is

there any possibility for galvanic corrosion to take place. To investigate what happens in cases like this the NaCl soaked foams were used in this study.

For a galvanic cell to originate the anode and the cathode needs to be surrounded by an electrolyte. Though it is considered that the skin and the core of the sandwich composite are well bonded to each other, but still there may be some micro gaps in between them. And if the electrolyte somehow reaches the interface between the skin and the core a galvanic cell will be created. Again as we know composite materials especially composite sandwich structures are very easily prone to damage. So if any how a composite sandwich structure is damaged which leads in creating a gap between the skin and the core, this may be a spot where corrosion can easily take place. In this case the bare core can also come in contact with the environment leading to corrosion.

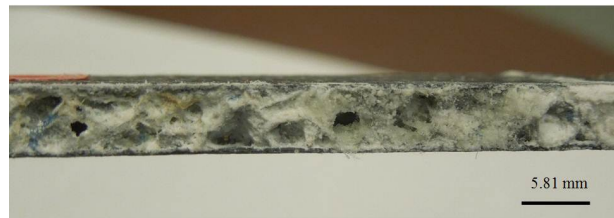


Figure 6.4: Corrosion test samples with dried salt layer before cleaning.

The sides of the samples had salt layers over it when taken out from the foams containing the NaCl solution. So it was necessary to clean the samples before taking the readings. The samples were cleaned with alcohol water solution and then dried properly. To keep the samples in a single position while taking the measurement the samples were held using a vise. Pieces of balsa wood were placed inside the vise to prevent direct contact of the specimens with the metallic walls of the vise.

# CHAPTER 7: RESULT AND DISCUSSION

## 7.1 Flexural Test Findings

In sandwich composite structures the core is an very important component in enhancing the flexural rigidity of the system and in controlling the failure mechanisms. And for sandwich beams with foam core, the performance of the system under flexural load depends mainly on the strength of the core material and the de-bond strength at the core-skin interface [70]. One of the main advantages observed from the carbon fabric/epoxy-aluminum foam sandwich structure is that it has a very high skin-core de-bonding resistance [15]. Both flexural test and corrosion test proofed that there exists a very strong interfacial bond in these sandwich structures.

In flexural test the skins of a sandwich composite takes almost all the compressive and tensile stresses. That is why for sandwich beams with thin skins under flexural load, the skins easily fail in face yield mode. As the core of the sandwich beams are sufficiently thick, initially they undergo an indentation mode but eventually with further flexural deflection the sandwich beams collapse in a face yield failure mode [34].

So it can be seen from the three point flexural test of sandwich beams with aluminum foam core that the load deflection curve exhibits three distinct zones. The curve first exhibits a region of nearly linear elastic behavior of the sandwich beam which takes place at low deflection; followed by a region where a rapid drop in load occurs once the load exceeds the yield point; and finally a plateau region with slight fluctuation in load over a wide range of the large deflection values occur [37].

The three point flexural test of the carbon fabric/epoxy-aluminum foam sandwich beams also gave a force versus displacement plot with three distinct regions. In the first region the load value increased with increase in deflection, then there was a large drop in the load carrying capacity of the beams due to failure of the top skin. As the load of the beam was transferred from the top skin to the core the large sudden drop stopped at a much smaller force value which was followed by a plateau region. Then with further displacement core crushing lead to core densification, which is indicated by a slight rise in the load bearing capacity of the structure.

Though fiber breakage and matrix cracking of the top skin occurred but not much delamination was observed. Even after going through a large displacement the skins were strongly bonded with the core and



at the initial stage of the flexural process the skins were seen to be strongly bonded with the core, which indicates that the samples have a very good interfacial bond strength. Very less damage was observed at the lower skin.

The delamination occurs mostly under the point of contact. And it occurs within a very small area. Though the flexural displacement progresses the delamination does not progress much. But for samples (only few) where the top skin fails at a place not directly under the point of contact but a little side to it, the delamination size in these cases are larger compared to the samples where the top skin failure occurs directly under the point of contact. For the carbon fabric/epoxy-aluminum foam samples the delamination occurred in the skin core interface. No delamination occurred between the individual plies of the skins. For the carbon fabric/epoxy-GFRP-aluminum foam samples the delamination occurs at the interface of carbon fabric plies and GFRP ply. Not much delamination is observed between the GFRP and the core. As the aluminum foam has a very rough surface the interfacial bonding between the core and the skins are very strong. So despite it going under high displacement the initial delamination size does not propagate much. And due to this strong interface bonding the delamination for the carbon fabric/epoxy-GFRP-aluminum foams occur more at the carbon fabric-GFRP interface rather than occurring in the GFRP-aluminum core interface.

## 7.2 Influence of Barrier Layer on Beams Mechanical Properties

### 7.2.1 Damage Location

#### For Type A Samples

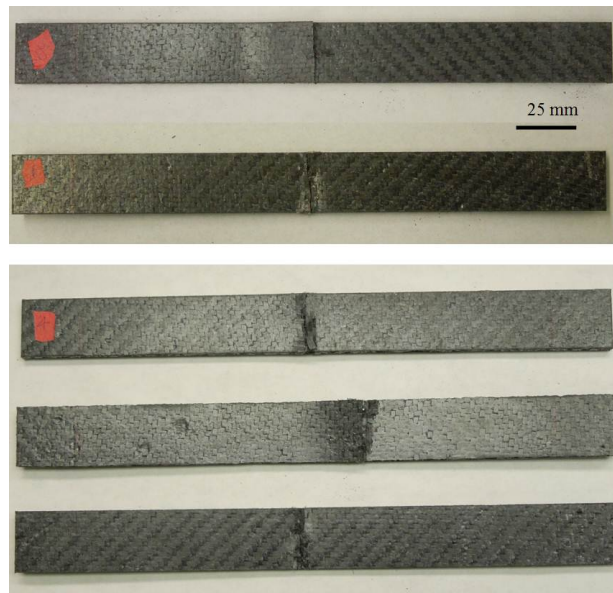


Figure 7.1: Damage location of type A samples.

#### For Type B Samples

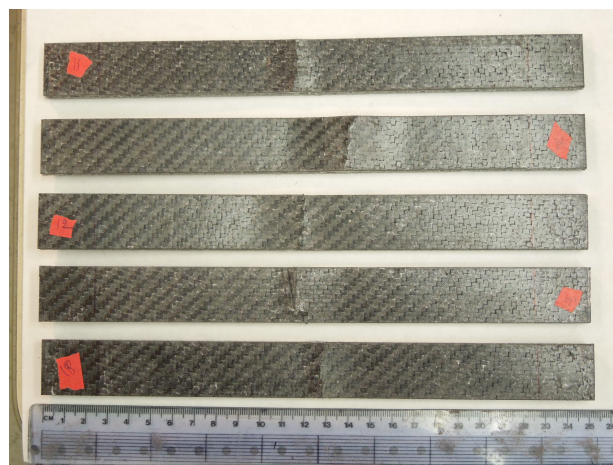


Figure 7.2: Damage location of type B samples.

From both of the damaged sample types it is seen that in most of the samples the top skin fails at a area

directly in contact with the loading pin, which is at the center of the specimens. Only for a few samples damage of the top skin occurs at a location not directly under the ball, but at a little distance to it at any of the sides.

### 7.2.2 Size of Delamination Area

The flexural test samples at the end of the test were straightened and the delamination size was measured. Type A sample had a delamination over an average length of 24.1 mm between the top skin and the core. And for the bottom skin and core the delamination occurs over an average length of 13.5 mm.

For type B samples for the top skin the delamination takes place at the interface of carbon fabric/epoxy plies and the GFRP layer and between the GFRP layer and the core. And for the bottom face the delamination only takes place between the interface of GFRP and the core. For the top skin the delamination length between the plies of carbon fabric/epoxy and the GFRP interface is of 22.5 mm and that between the GFRP and the core interface is over the length of 7.9 mm. And for the bottom skin the length over which the delamination between the GFRP and core interface occurs is 5.2 mm.

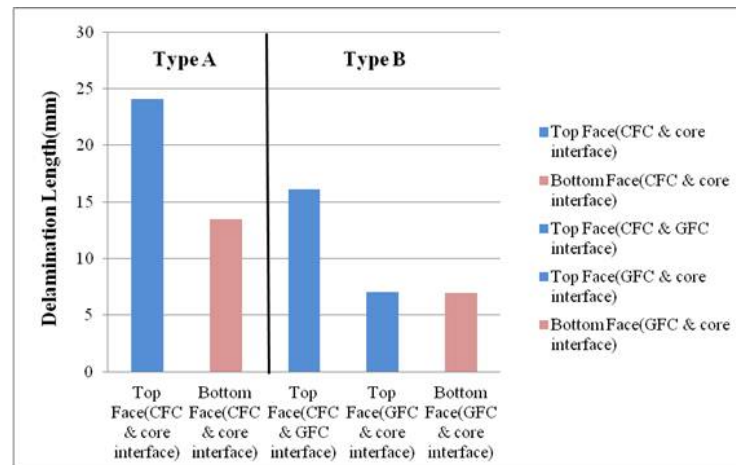


Figure 7.3: Delamination area of type A and type B samples.

### 7.2.3 Permanent Central Deflection

After removing the load from the tested samples their permanent deflection at the center was measured. Type A sample had a permanent central deflection of  $4.94 \pm 0.47$  cm and for type B samples it was  $2.43 \pm 0.41$  cm. It was found that type A samples without the GFRP layer in between the carbon fabric/epoxy

plies and the core under went more deflection than the type B samples having the GFRP layer. This is because the GFRP layer is increasing the thickness of the total composite beam which is increasing its moment of inertia. Thus increasing its flexural rigidity. Therefore, type B samples having less central deflection.

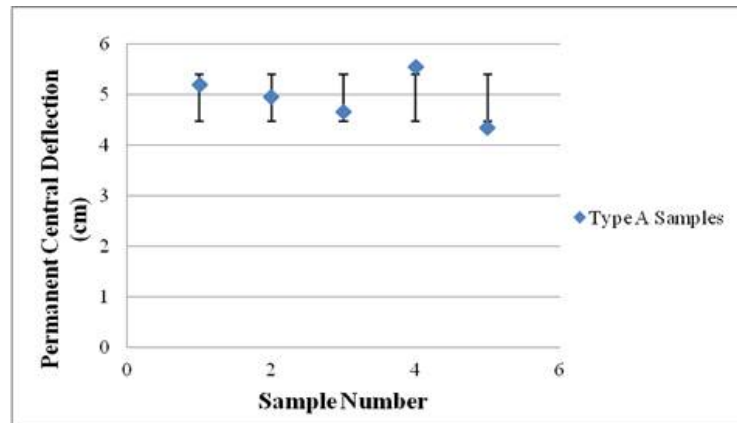


Figure 7.4: Permanent central deflection of type A samples with standard deviation from the mean value.

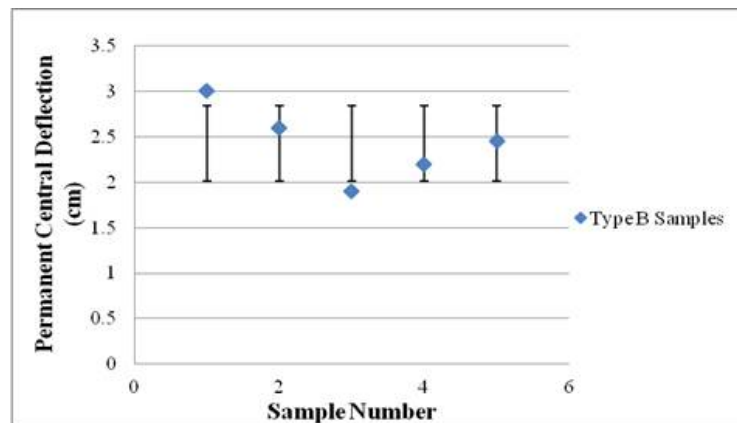


Figure 7.5: Permanent central deflection of type B samples with standard deviation from the mean value.

Organizing the permanent deflection in an ascending order and plotting against number of samples, the following plot is obtained. Sample A undergoes more deflection due to less flexural rigidity because it has less thickness compared to type B samples.

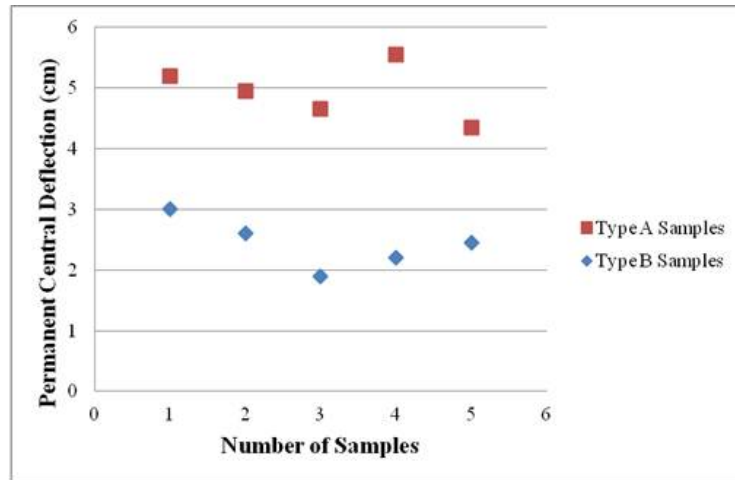


Figure 7.6: Comparison of permanent central deflection between type A and type B samples.

### 7.3 Corrosion Test Findings

There are various techniques to monitor corrosion, some can measure corrosion rate directly, while some techniques only indicates that corrosive is taking place [69]. In this study the method of corrosion monitoring through change in electrical resistance indicates whether the sandwich composite core is undergoing corrosion or not. This is a non destructive way of predicting corrosion, no harm is done to the sandwich structure.

Corrosion damages the samples core, which ultimately damages the whole structural circuit, leading to an overall increase in resistance. Though this increase in resistance cannot very easily be directly correlated to corrosion rate [64]. But this increase in resistance can be a very useful tool to monitor the condition of a sandwich composite core. And like other corrosion monitoring techniques this method can be helpful in providing an early warning that the core is being damaged due to corrosion, so that necessary preventive steps can be taken in time to avoid corrosion-induced failures [65].

Again this technique can be very useful in the sense that it is very simple to understand and implement and at the same time it can offer significant economic benefit to the user as it can monitor corrosion while the sandwich composite is still in service, thus reducing service down time and also helping in extending the life of the structure [65].

The type A and type B specimens were exposed to different environmental conditions under different boundary conditions. After a certain time of exposure each sample was properly dried and the electrical

resistance of the cores were measured using the four probe electrode method. The resistance values were plotted against the duration of exposure in terms of days. Some variation in the resistance value was observed due to presence of electrical noise in the reading. Pictures of the cores were also taken and were correlated with the resistance vs time plots. It is seen that a good co-relation was observed between the plots and the pictures regarding the presence of corrosion.

Initially the samples were kept in room environment to monitor its behavior in terms of electrical resistance measurement in this atmosphere. After being exposed to room environment for a 72 days, most of the samples were then exposed to the aggressive environment. Only a few were still kept in the room atmosphere.

The pictures below show the condition of the sample cores after 72 days of exposure in normal room environment. It is seen that for both type A and type B sample no change occurred to the cores. Even the resistance change over time showed no significant rise of the core resistance.



Figure 7.7: Type B unsealed sample after 72 days exposure in room atmosphere.



Figure 7.8: Type A unsealed sample after 72 days exposure in room atmosphere.

Then the samples were exposed to aggressive NaCl solution. It was seen that for some of the type B samples within a few days of exposure to NaCl solution small areas were showing presence of corrosion product. After 16 days of exposure the picture of the samples are shown below.

Unsealed type B samples after being exposed to NaCl solution for 16 days, it is seen that corrosion product developed over the uncovered sides of the sample. But for type A unsealed specimens after being

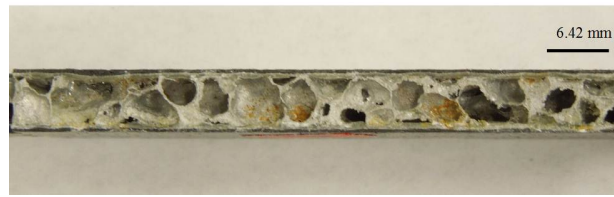


Figure 7.9: Type B unsealed sample after exposure to NaCl solution for 16 days.

exposed for the same duration in the NaCl solution no visible sign of corrosion was found.

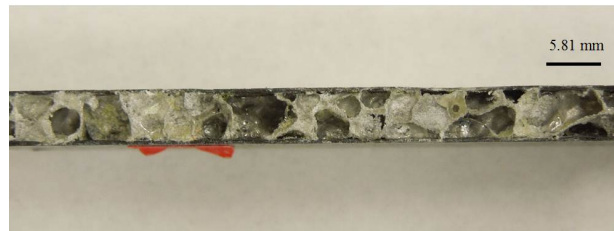


Figure 7.10: Type A unsealed sample after exposure to NaCl solution for 16 days.

The sample were than further exposed to NaCl Solution upto 70 days. Then the samples were taken out of the aggressive environment to investigate the condition of the sample core. Before taking pictures the sample cores were cleaned properly to get rid of the salt layer and then dried.

### Unsealed Carbon Fabric-Al Foam Sandwich Composite with GFRP Layer:

The type B unsealed samples shows two different behaviors from the resistance versus time curve. For all samples under this category during the period in which they were kept in the ambient atmosphere there was no significant change in the resistance. But as soon as the same samples were exposed to the aggressive NaCl solution, for some samples there was an rapid increase in the resistance value over time indicating corrosion taking place.

Also from the pictures of carbon fabric-aluminum foam sandwich composites specimens containing the GFRP barrier layer in between that were not sealed from the side it was found that after being exposed to the NaCl aqueous solution patches of small dark brown corroded spots where found in the surface of the exposed parts. This explains why the resistance versus time curve for these specimens had an upward nature when exposed to the NaCl solution.

For these samples after 16 days of exposure to aggressive environment brown patches of corrosion product was found on the core. After 70 days of exposure to the same environment that the size of the corroded area had not increased much over time but the color of the corroded area had turned darker.

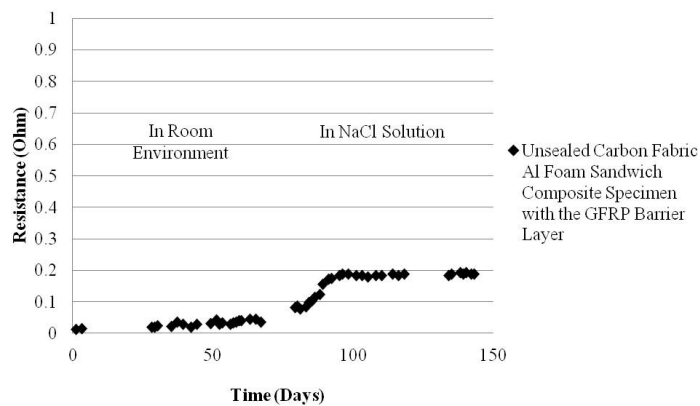


Figure 7.11: Typical resistance versus time plot for unsealed type B samples (first type of behavior).



It is seen from the above plot that for the region where the samples are exposed to NaCl solution the rise in the samples core resistance only takes place within the first 15-20 days of exposure. Then the resistance value with time again nearly becomes constant but remains at a higher resistance value than it was initially.

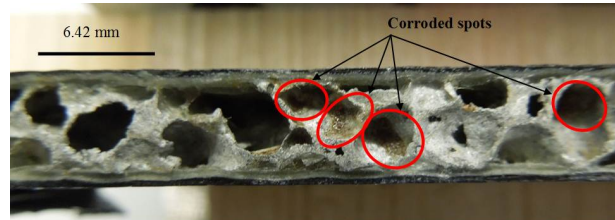


Figure 7.12: Unsealed type B sample core after being exposed to NaCl solution for 70 days (first type of behavior).

But for the same type of samples another type of behavior was observed. The resistance value did not change during the period the samples were exposed to the room environment. But even after being exposed to the aggressive NaCl solution there was not much change in the resistance value over time. So for the overall duration of exposure in different environments the resistance value remained quite the same.

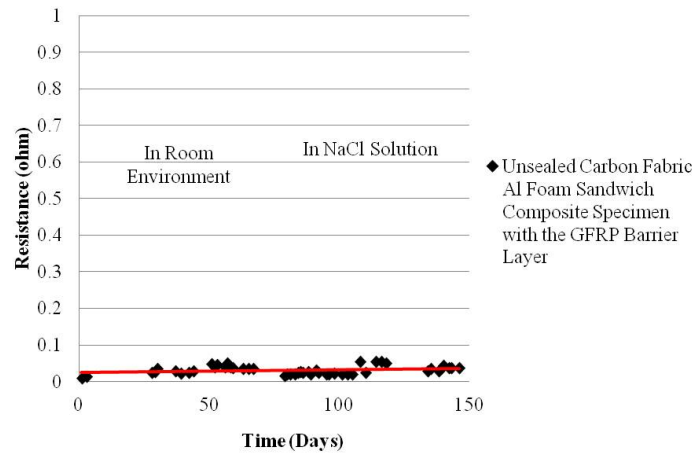


Figure 7.13: Typical resistance versus time plot for unsealed type B samples (second type of behavior).

But the corresponding sample core pictures showed that due to exposure in NaCl solution discoloration of the core occurred (core turned a little blackish) and small black spots over little areas were also found. This small black spots and discoloration are initial indication of corrosion taking place in the core. If

these type of samples were kept in the aggressive environment for a longer period of time, rise in the core resistance value over time would have been noticed.

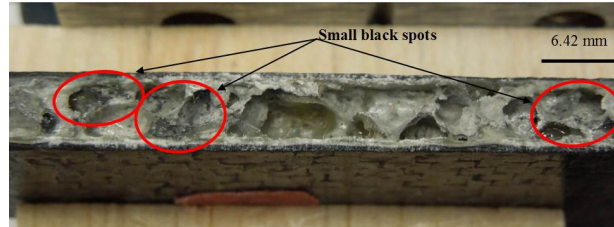


Figure 7.14: Unsealed type B sample core after being exposed to NaCl solution for 70 days (second type of behavior).

### Sealed Carbon Fabric-Al Foam Sandwich Composite with GFRP Layer:

For the sealed type B samples the resistance versus time curve shows that in both the environments i.e. in room atmosphere and in NaCl solution there was no significant change in the resistance of the core

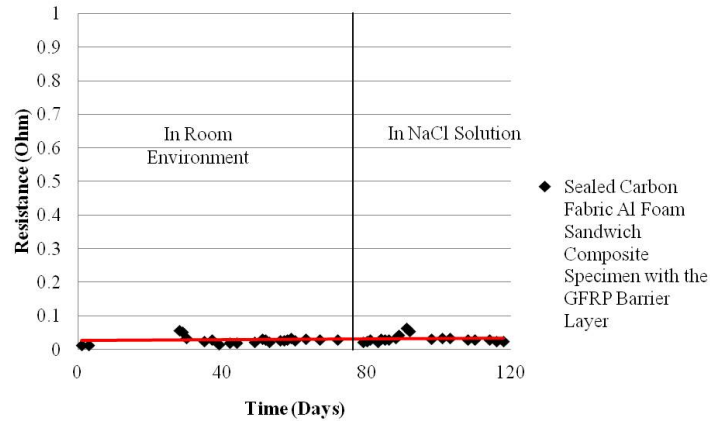


Figure 7.15: Typical resistance versus time plot for sealed type B samples.

For the type B sealed samples to inspect the condition of the core underneath the sealing layer, the sealing material was removed. As the Al foam surface had many pores it was not possible to remove the sealing material completely. Some of the material was stuck in the pores. Regardless of this the core under the sealing material could be clearly seen. It was seen that even though being exposed to the NaCl solution the core was the same as it was originally. No salt deposition or no sign of corrosion product was found. So both from the resistance plot and the core pictures it can be said that, no corrosion took place in the core for sealed type B samples.



Figure 7.16: Peeled core of sealed type B sample.

But after removing the seal layer from one of the type B samples it was seen that patches of salt was found under the sealant layer. This is because though a layer of epoxy was applied on top of the silicon chalk, as the chalk layer had a rough surface it was not holding the epoxy layer properly, so the epoxy layer were breaking in small pieces and falling off. And it was noticed that after being exposed to the

aggressive NaCl environment for some time, the chalk layer was wearing out and becoming thin. This lead to small cavities in the sealant layer allowing some of the electrolyte solution to enter through the sealant and come in to contact with the core material. As the silicon chalk used was water proof so it is considered that no electrolyte solution had been absorbed through it.

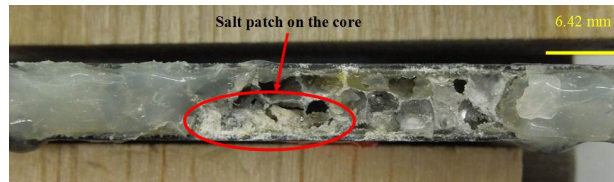


Figure 7.17: Peeled core of sealed type B sample with salt patches.

### Unsealed Carbon Fabric-Al Foam Sandwich Composite:

The resistance versus time curve for the unsealed type A samples also showed that there was no significant change in the core resistance over time for the sample while being kept in both the environments.

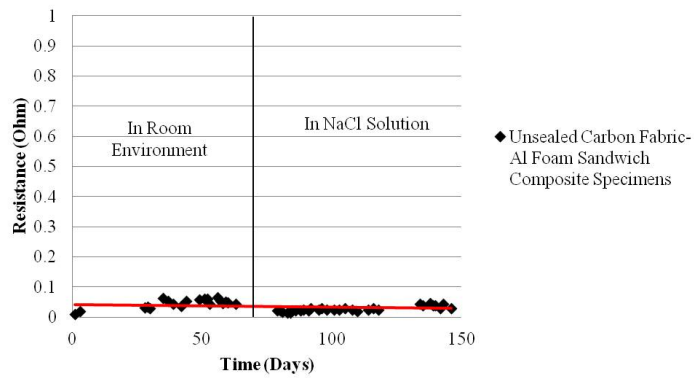


Figure 7.18: Typical resistance versus time plot for unsealed type A sample.

After being properly cleaned it was seen that for unsealed type A samples there was no sign of any corrosion product on the core of the samples. Also for this type of samples nearly the entire core was covered with epoxy layer which was produced from the pre-preg carbon fabric/epoxy plies during the manufacturing process.



Figure 7.19: Unsealed type A sample core.

### Sealed Carbon Fabric-Al Foam Sandwich Composite:

The resistance versus time curve for the sealed type a sample core also nearly represents a straight line indicating that in both the environments not much of a change happened to resistance of the core. Which means that for this type of sample while exposed to NaCl environment no galvanic corrosion had taken place.

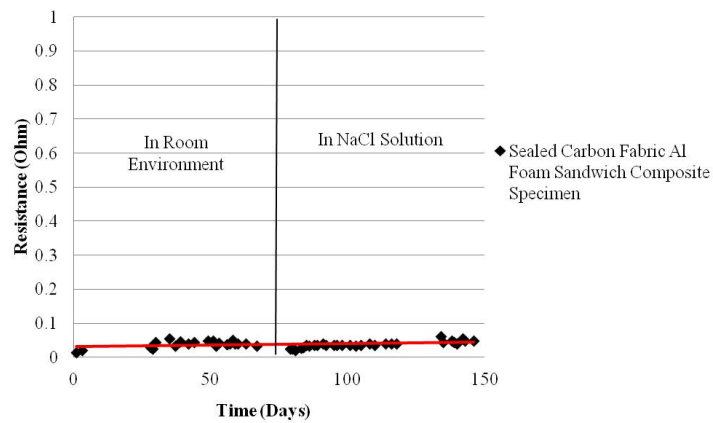


Figure 7.20: Typical resistance versus time plot for sealed type A sample.

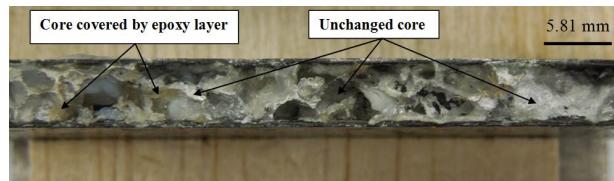


Figure 7.21: Sealed type A sample core.

After removing the sealant layer it was seen that the core of this type of sample even after being exposed to aggressive environment for a sufficient amount of time the core has not undergone any change. There is no sign of any corrosion product. Most part of the core was covered by an epoxy layer generated from the skin during the curing process.

**Carbon Fabric-Al Foam Sandwich Composite with GFRP Layer Exposed to Atmospheric Condition:**

Resistance versus time plot shows that the core resistance for this kind of samples in the room environment merely remains the same.

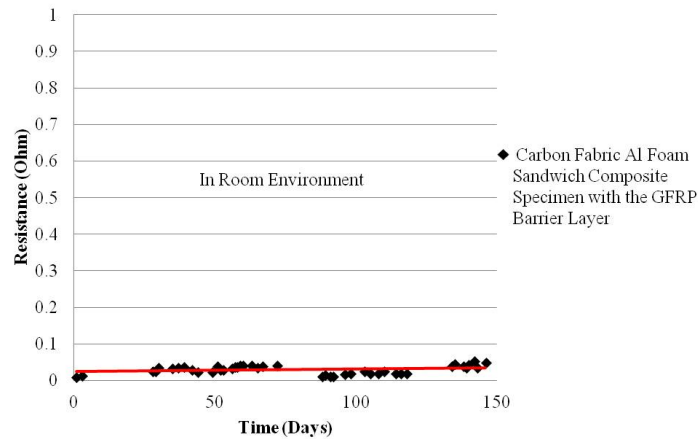


Figure 7.22: Typical resistance versus time plot for unsealed type B samples kept in room environment.

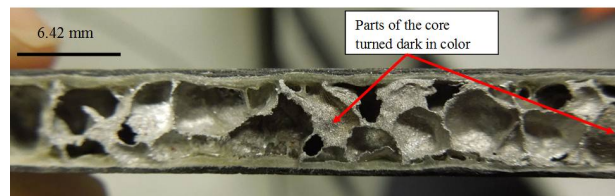


Figure 7.23: Core of unsealed type B sample kept in room environment.

The picture of the core for type B unsealed samples shows that after being kept in the room environment for 146 days, no corrosion product was found on the core. Only some part of the core has lost its original silvery color and turned a little dark.

### Carbon Fabric-Al Foam Sandwich Composite Exposed to Atmospheric Condition:

For type A unsealed samples the resistance versus time curve shows no change in resistance with time. The picture of the core also shows no change. Even after being exposed to the room environment for 146 days the core is still as same as it was originally. So this indicates for this type of samples kept in room environment no change occurs to the core i.e no corrosion takes place.

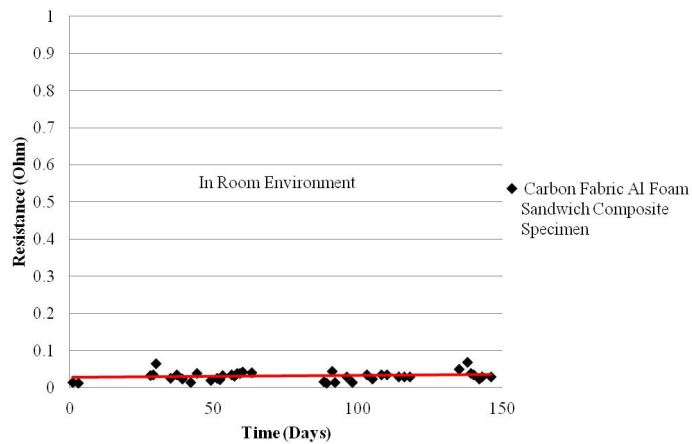


Figure 7.24: Typical resistance versus time curve for type A unsealed samples kept in room environment.

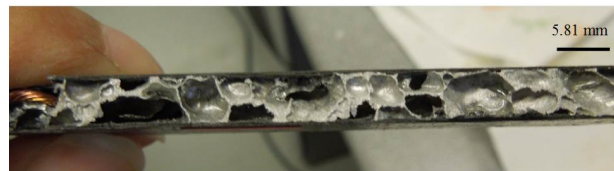


Figure 7.25: Core of type A unsealed sample after being kept in room environment.

Due to the high potential difference between carbon and aluminum, if the carbon fabric/epoxy-aluminum foam sandwich beams are exposed to any electrolyte the system may create a galvanic cell leading to corrosion of the aluminum foam core. Barrier layer was used in between the carbon fabric skin and aluminum foam to break the connection between the skin and core, thus preventing galvanic corrosion to take place. But it was seen from the resistance change versus time plot and pictures of the cores, that for the carbon fabric aluminum foam sealed and unsealed samples exposed to NaCl solution no corrosion is taking place. But for some of the unsealed samples with the barrier layer shows sign of corrosion taking place both from the resistance plot and the pictures. The unsealed type B samples (samples with the barrier layer) when



exposed to the NaCl solution the barrier layer is absorbing the solution and creating a salt bridge between the carbon cathode and aluminum anode, thus creating a galvanic cell. But the sealed type B samples showed no sign of corrosion.

So to prevent galvanic corrosion inserting a barrier layer between the anode material and the cathode material is not enough, the system also needs to be insulated from the surrounding so that the barrier material cannot come in contact with the electrolyte solution.

For these sandwich systems comprising of carbon fabric/epoxy skin and aluminum foam core the interfacial bond is so strong and the skin pre-preg plies during curing crates an epoxy layer over the exposed parts of the core. This phenomenon is prominent in type A samples and this epoxy layer plays a role in protecting the metal core from being corroded. The results show that, for these systems extra barrier layer does not show any benefit in corrosion protection. And the efficient way of protecting these structures from galvanic corrosion is by sealing the bare ends of the core to prevent any electrolyte coming in contact with this dissimilar metal system.

## CHAPTER 8: COMPARISON STUDY

Under a different project the behavior of composite sandwich beam made of unidirectional carbon fiber/epoxy skin and aluminum core in corrosion inducing aggressive media and its effect on the mechanical properties of the system was investigated. Some of the results obtained from that study is shared here.



Figure 8.1: Unidirectional carbon fiber/epoxy skin and aluminum core sandwich specimen with electrical connections to measure core resistance.

The samples were prepared using the autoclave type vacuum press and no additional adhesive was used at the interface. To improve the bonding between the skin and core, sand paper was used to create a rough cross hatch surface on the aluminum core.

As the corrosion inducing media 3.5 wt% NaCl water solution was used. This is the same concentration of NaCl solution the carbon fabric/epoxy-aluminum foam sandwich beams were exposed to. So both the sandwich beams, the ones made of aluminum foam core and the ones having aluminum core were exposed to the same aggressive media. But the carbon fabric/epoxy pre-preg had slightly less fiber volume fraction than the unidirectional carbon fiber/epoxy pre-pregs. Which means that the carbon fabric/epoxy pre-pregs contained more epoxy than the unidirectional carbon fiber/epoxy pre-pregs.

The aluminum core samples were exposed to the aggressive NaCl environment only for 15 days. Within this short period of time the samples were quite badly affected by the chloride atmosphere, which is discussed below with some picture of the cores.

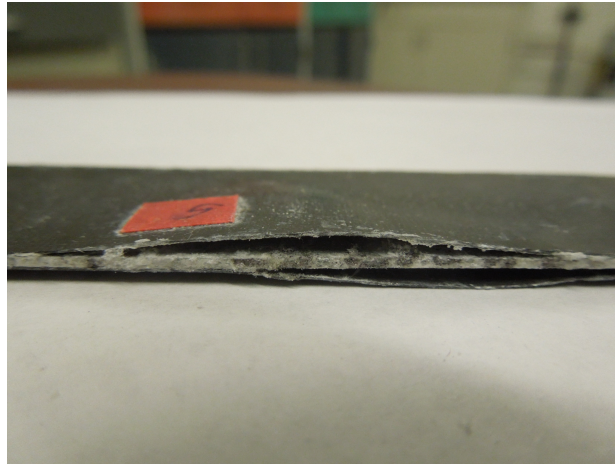


Figure 8.2: Exposure to NaCl solution causing delamination between the core and skin.

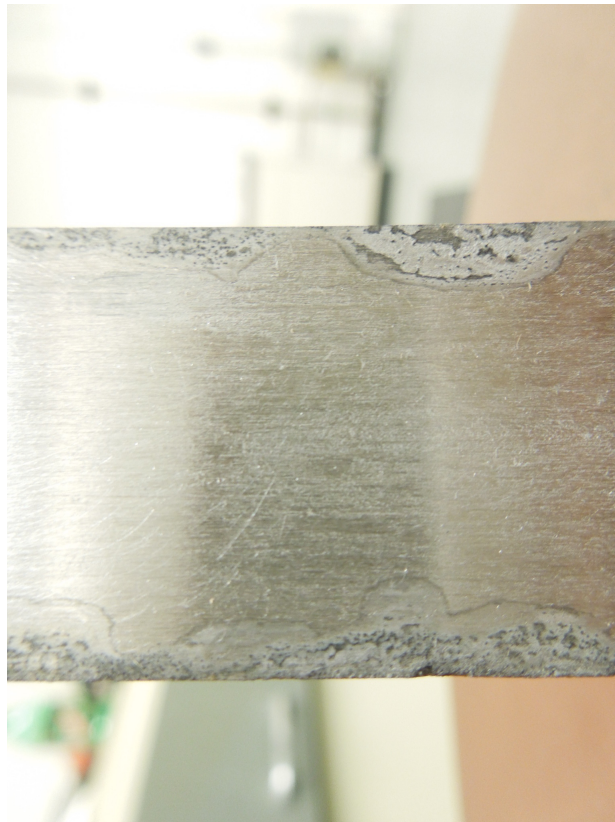


Figure 8.3: Aluminum core sides corroded due to delamination allowing the sandwich samples to be exposed to the NaCl solution.

From the pictures it can be seen that though the unidirectional carbon fiber/epoxy-aluminum sandwich samples were kept in the aqueous NaCl solution for only 15 days, but it had a very adverse affect on

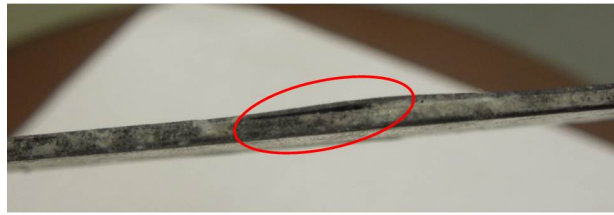


Figure 8.4: Delamination on one side of the core.

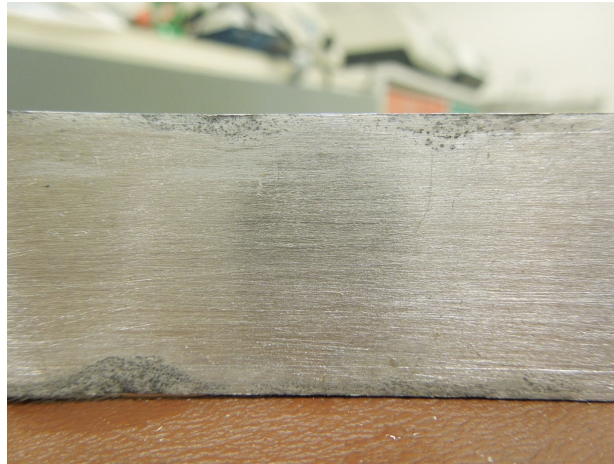


Figure 8.5: Core corroded in the areas of sample undergoing delamination.

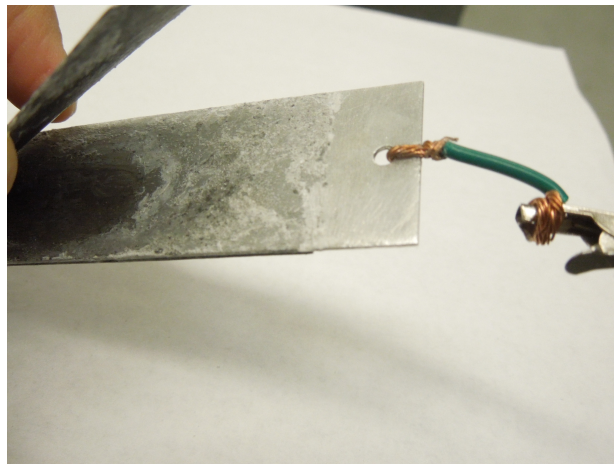


Figure 8.6: Skin separated from core due to exposure of NaCl solution.

the samples. The NaCl solution was weakening the bond between the skin and core interface gradually leading to delamination. For some samples the delamination took place on both side of the core and for some sample it only took place at one side of the core. These delamination were creating an opening



Figure 8.7: Corrosion product on core after removing the skin totally and cleaning the core of above figure.

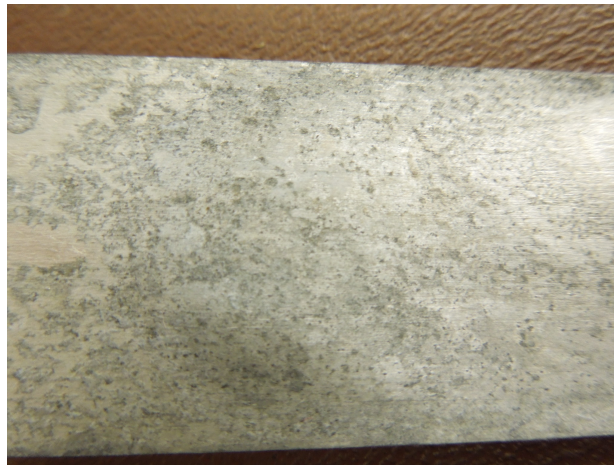


Figure 8.8: Closer look at the corroded core of above figure.

for the NaCl to come in contact with the bare aluminum core. The carbon fiber skin and the core was in contact at some places and at the same time these delaminated spots allowed the NaCl to enter between the skin and core, thus fulfilling all the conditions required to create a galvanic cell. This lead to quite severe corrosion of the core at those spots.

For some samples due to the presence of the NaCl solution the skin was simply separating from the core, thus again exposing a large part of the core to the NaCl solution leading to corrosion.

Now comparing these result between the sandwich beams made using aluminum foam it is seen that, both samples were prepared using no additional adhesive at the interface and both were exposed to 3.5 wt% NaCl solution. The aluminum core samples were exposed in the aggressive environment for 15 days

only and the aluminum foam core samples were exposed for 70 days. Within this 15 days of exposure the aluminum core samples showed skin-core delamination and also core to skin separation. Thus allowing the NaCl solution to directly come in contact with the bare aluminum core and leading to corrosion of the core. The aluminum foam core samples were exposed to the same environment for 70 days but still the skins were very strongly bonded to the core. To inspect the core under the skin, the skin was tried to be removed from the aluminum foam core. But due to this strong bond at the interface it was impossible to remove the skin from the core without damaging the sample. So the NaCl solution was not able to weaken the interfacial bond for this kind of samples. No delamination or core to skin separation was observed for the foam samples.

Therefore, it can be said that the rough surface of the aluminum foam core provides it with the advantage of having a very strong interfacial bonding at the skin core interface. Reducing the possibility of any gap or weak spot at the interface and protecting the samples against galvanic corrosion.

## CHAPTER 9: CONCLUSION

Sandwich composite structure made of aluminum foam has the advantage of very strong bond between the skins and the core at the interface. Strong interfacial bond for these sandwich structures improves its mechanical performance and also helps in getting better protection against corrosion. Aluminum foam cores when bonded with carbon fabric/epoxy pre-preg plies, the composite plies while curing creates an adhesive layer at the interface and this adhesive layer also overflows covering a great portion of the exposed sides of the foam core. This provides the carbon fabric/epoxy-aluminum foam structures an advantage in preventing corrosion in a chloride-enriched environment, as most parts of the core are covered by an insulating epoxy layer. Instead of aluminum foam, sandwich structures made of aluminum core when exposed to aggressive corrosion-inducing media, within a short period of exposure experience weakening of the interfacial bond. Thus exposing the aluminum core to the chloride environment which leads to corrosion in the core. But this is not the same case for the sandwich beams made of aluminum foam cores. Samples with aluminum foam core exhibited a very strong bond at the skin-core interface even after exposure to aggressive NaCl aqueous environment for a sufficient amount of time. The unsealed carbon fabric/epoxy-aluminum foam sandwich beam did not show any significant rise in the resistance of the core over time, indicating no damage occurrence in the core due to corrosion. But the pictures of the exposed core showed some change in color and a very little black spot, which is an early indication of corrosion. To avoid this risk, it is better to insulate the exposed parts of the core from the environment. As for the sealed carbon fabric/epoxy-aluminum foam samples, the resistance versus time plot did not show any change in the core resistance over time, and the core also did not show any visual change. So galvanic corrosion in these samples can be easily prevented by not allowing any electrolyte to come in contact with the dissimilar material system by sealing all the exposed parts of the core.

For carbon fabric/epoxy-aluminum foam structures with the glass fiber epoxy-based barrier layer, it does not appear to protect the structure from galvanic corrosion in an aggressive environment. On the other hand, most samples with the barrier layer in the NaCl environment show a rapid rise in the resistance of the core with time. And also the picture of the exposed cores shows the existence of corrosion. One of these samples did not show any significant increase in the core resistance with time in the aggressive media. But the core showed small dark spots and decolorization, which are initial indications of corrosion taking

place. If this sample is exposed to the NaCl solution for a further period of time the corrosion rate will increase leading to an increase in the core resistance over time. These unsealed carbon fabric/epoxy-aluminum foam sandwich beams with the barrier layer when exposed to the NaCl environment, the glass fiber epoxy based barrier layer absorbs the chloride solution from the exposed sides and works as a salt bridge between the carbon fabric skin and aluminum foam, thus creating a galvanic cell. So the use of barrier layers in these samples without insulating the structure from the surrounding environment may not be a good solution in preventing galvanic corrosion.

It is obvious from the flexural test that the carbon fabric/epoxy-aluminum foam sandwich samples with the barrier layer have higher flexural rigidity and more load carrying capacity than the ones without the barrier layer. So if the application of the structure requires higher load bearing capacity than the use of the samples with the barrier layer makes sense. But if the purpose of using the barrier layer is to prevent galvanic corrosion in these sandwich structures, then from this study it can be concluded that the epoxy based barrier layer does not provide corrosion protection as one would customarily think. The carbon fabric/epoxy-aluminum foam sandwich structures can be protected from galvanic corrosion just by insulating all the exposed core parts of the structure from the surrounding environment.

From this study the following conclusions can be made,

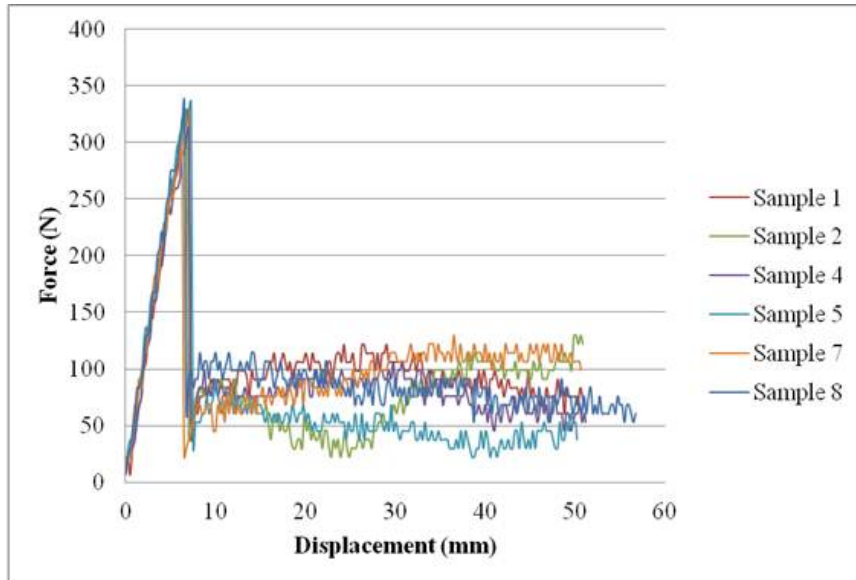
1. Aluminum foam provides a very strong interfacial bond.
2. Carbon fabric/epoxy skin during curing creates an epoxy layer over the exposed parts of the core, protecting them from the surrounding environment. Specially in type A samples (carbon fabric/epoxy-aluminum foam samples without the glass fiber/epoxy based barrier layer).
3. Use of glass fiber/epoxy based barrier layer to break contact between the aluminum anode and carbon cathode is not effective in preventing galvanic corrosion in these samples as it creates a salt bridge between the skin and core.
4. Sealing these samples from the environment in order to not allow any electrolyte solution to come in contact with the dissimilar material system is the best solution for galvanic corrosion protection.



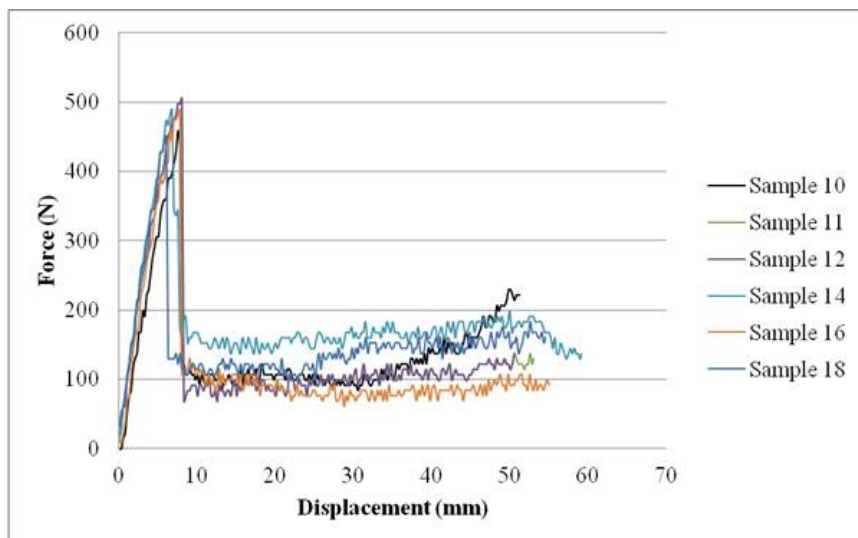
## **CHAPTER 10: FUTURE WORK**

1. From the rise of resistance over time rate of corrosion can be determined.
2. Relation between corrosion rate and its influence on mechanical properties can be investigated.
3. Fatigue test can be conducted to evaluate the durability of these samples under stages of corrosion.
4. Electron probe spectroscopy and other established methods can be run at the same time to investigate and compare the results.

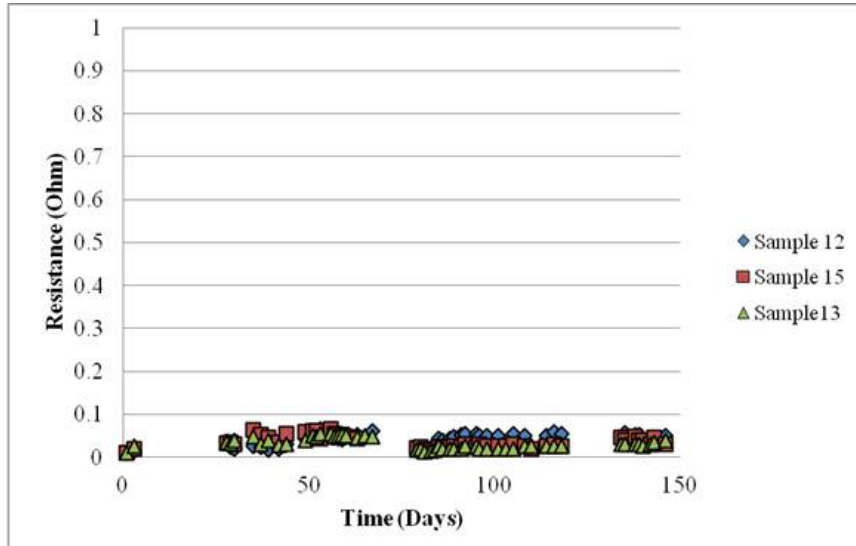
## APPENDIX



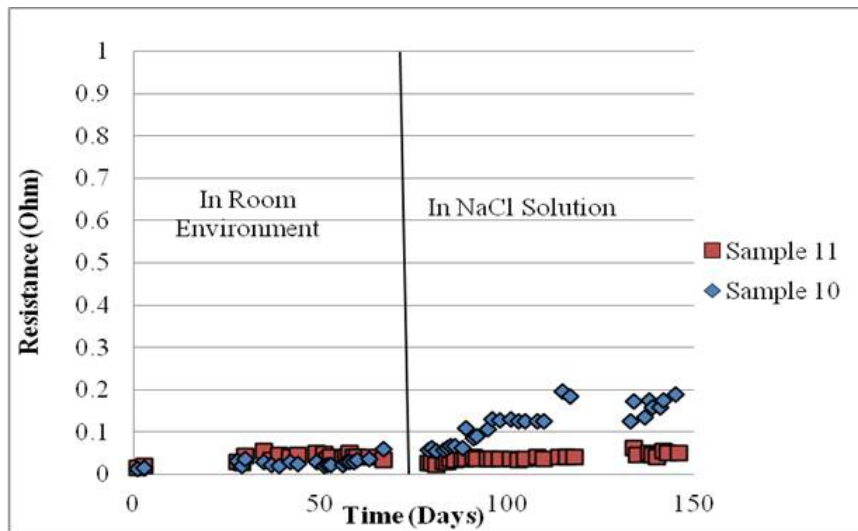
Force vs displacement plot for type A samples under three point flexural test.



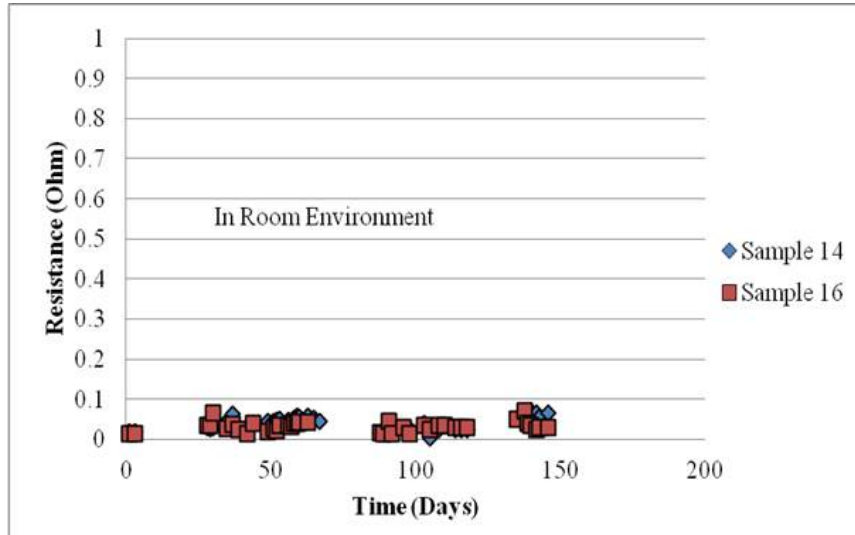
Force vs displacement plot for type B samples under three point flexural test.



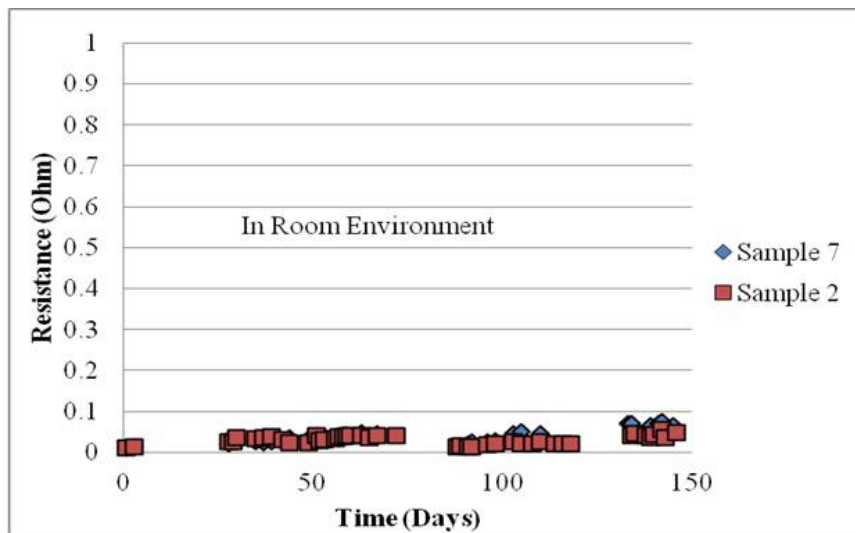
Resistance versus time plot for unsealed Type A samples in NaCl solution.



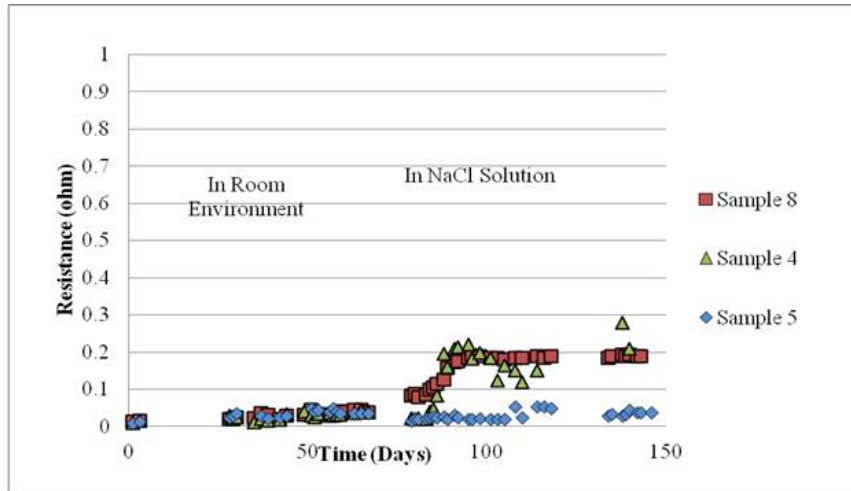
Resistance versus time plot for sealed Type A samples in NaCl solution.



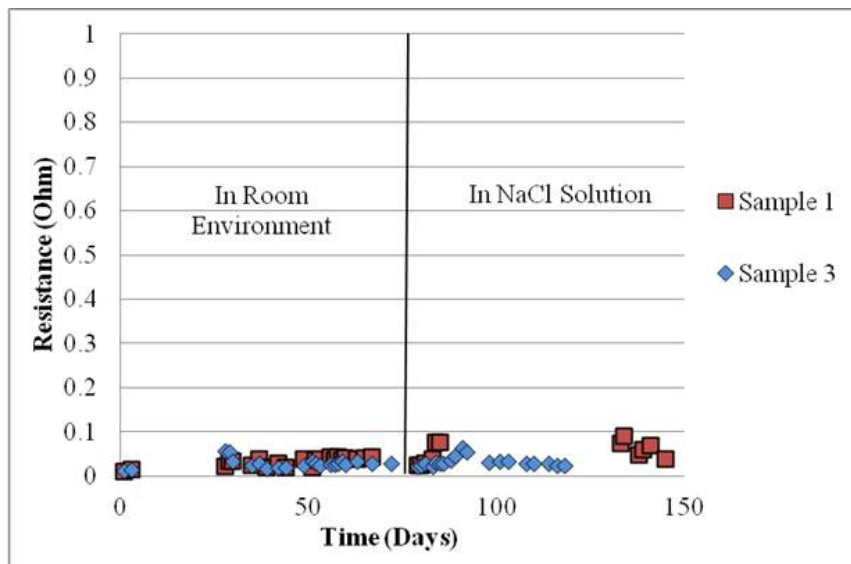
Resistance versus time plot for type A unsealed samples kept at room atmosphere.



Resistance versus time plot for type B unsealed samples kept at room atmosphere.



Resistance versus time plot for Type B unsealed samples in NaCl solution.



Resistance versus time plot for Type B sealed samples in NaCl solution.

## REFERENCES

- [1] Po-Yu Chen, Joanna McKittrick, and Marc Andr Meyers. Biological materials: Functional adaptations and bioinspired designs. *Progress in Materials Science*, 57(8):1492 – 1704, 2012.
- [2] Avinash S. Phadatare. *Flexural analysis of balsa core sandwich composite: failure mechanisms, core grain orientation and padding effect*. PhD dissertation, 2012.
- [3] Mohan M. Ratwani. *Composite Materials and Sandwich Structures - A Primer*.
- [4] Rekha Rattan and J. Bijwe. Carbon fabric reinforced polyetherimide composites: Influence of weave of fabric and processing parameters on performance properties and erosive wear. *Materials Science and Engineering: A*, 420(12):342 – 350, 2006.
- [5] <http://www.stylepark.com/en/alcarbon/alporas-ac-black-both-sided-ground>.
- [6] John Banhart. Manufacture, characterisation and application of cellular metals and metal foams. *Progress in Materials Science*, 46(6):559 – 632, 2001.
- [7] <http://www.advancedmaterialsassoc.com/picts/electrochem%20galvanic%20corr.gif>.
- [8] K.S.C. Kuang, W.J. Cantwell, L. Zhang, I. Bennion, M. Maalej, and S.T. Quek. Damage monitoring in aluminum-foam sandwich structures based on thermoplastic fiber-metal laminates using fiber bragg gratings. *Composites Science and Technology*, 65(8):1800 – 1807, 2005.
- [9] [http://www.allaboutcircuits.com/vol\\_6/chpt\\_3/14.html](http://www.allaboutcircuits.com/vol_6/chpt_3/14.html).
- [10] Jin Dai and H. Thomas Hahn. Flexural behavior of sandwich beams fabricated by vacuum-assisted resin transfer molding. *Composite Structures*, 61(3):247 – 253, 2003.
- [11] Richard Stewart. Sandwich structures deliver core benefits. *Reinforced Plastics*, 54(4):32 – 37, 2010.
- [12] Venkata Dinesh Muthyala. *Composite sandwich structure with grid stiffened core*. PhD dissertation, 2007.
- [13] [http://www.angelfire.com/ma/ameyavaidya/F\\_sandwch3.htm](http://www.angelfire.com/ma/ameyavaidya/F_sandwch3.htm).

- [14] G. Pitarresi, J.J. Carruthers, A.M. Robinson, G. Torre, J.M. Kenny, S. Ingleton, O. Velecela, and M.S. Found. A comparative evaluation of crashworthy composite sandwich structures. *Composite Structures*, 78(1):34 – 44, 2007.
- [15] A.W van Vuure, J.A Ivens, and I Verpoest. Mechanical properties of composite panels based on woven sandwich-fabric preforms. *Composites Part A: Applied Science and Manufacturing*, 31(7):671 – 680, 2000.
- [16] Birsan, T. Sadowski, L. Marsavina, E. Linul, and D. Pietras. Mechanical behavior of sandwich composite beams made of foams and functionally graded materials. *International Journal of Solids and Structures*, 50(34):519 – 530, 2013.
- [17] Richard Stewart. Sandwich composites excel at cost-effective, lightweight structures. *Reinforced Plastics*, 55(4):27 – 31, 2011.
- [18] Gianni Nicoletto and Enrica Riva. Failure mechanisms in twill-weave laminates: Fem predictions vs. experiments. *Composites Part A: Applied Science and Manufacturing*, 35(78):787 – 795, 2004.
- [19] Sun-Pui Ng, Ping-Cheung Tse, and Kwok-Jing Lau. Numerical and experimental determination of in-plane elastic properties of 2/2 twill weave fabric composites. *Composites Part B: Engineering*, 29(6):735 – 744, 1998.
- [20] Ph. Vandeurzen, J. Ivens, and I. Verpoest. A three-dimensional micromechanical analysis of woven-fabric composites: Ii. elastic analysis. *Composites Science and Technology*, 56(11):1317 – 1327, 1996.
- [21] Yong-Ming Zhang, Xu-Ming Chu, Hui Wang, Si-Yuan He, and De-Ping He. Fabrication of almgre foams and their corrosion resistance properties. *Corrosion Science*, 51(6):1436 – 1440, 2009.
- [22] Arnaud Pollien, Yves Conde, Laurent Pambaguian, and Andreas Mortensen. Graded open-cell aluminium foam core sandwich beams. *Materials Science and Engineering: A*, 404(12):9 – 18, 2005.
- [23] M. Styles, P. Compston, and S. Kalyanasundaram. Finite element modelling of core thickness effects in aluminium foam/composite sandwich structures under flexural loading. *Composite Structures*, 86(13):227 – 232, 2008. *Fourteenth International Conference on Composite Structures/ICCS/14*.

- [24] V. Crupi and R. Montanini. Aluminium foam sandwiches collapse modes under static and dynamic three-point bending. *International Journal of Impact Engineering*, 34(3):509 – 521, 2007.
- [25] AH Brothers and DC Dunand. Amorphous metal foams. *Scripta Materialia*, 54(4):513–520, 2006.
- [26] W.J. Cantwell, P. Compston, and G. Reyes. The fracture properties of novel aluminum foam sandwich structures. *Journal of Materials Science Letters*, 19(24):2205–2208, 2000.
- [27] G. Reyes Villanueva and W.J. Cantwell. The high velocity impact response of composite and fml-reinforced sandwich structures. *Composites Science and Technology*, 64(1):35 – 54, 2004.
- [28] Paul Compston, Millicent Styles, and Shankar Kalyanasundaram. Low energy impact damage modes in aluminum foam and polymer foam sandwich structures. *Journal of Sandwich Structures and Materials*, 8(5):365–379, 2006.
- [29] [http://www.alfed.org.uk/downloads/documents/NEXCLVIUKN\\_2\\_aluminium\\_and\\_corrosion.pdf](http://www.alfed.org.uk/downloads/documents/NEXCLVIUKN_2_aluminium_and_corrosion.pdf).
- [30] <http://www.aluminiumdesign.net/design-support/aluminiums-corrosion-resistance/>.
- [31] ZF Yin, ML Yan, ZQ Bai, WZ Zhao, and WJ Zhou. Galvanic corrosion associated with sm 80ss steel and ni-based alloy g3 couples in nacl solution. *Electrochimica Acta*, 53(22):6285–6292, 2008.
- [32] R Akid and D.J Mills. A comparison between conventional macroscopic and novel microscopic scanning electrochemical methods to evaluate galvanic corrosion. *Corrosion Science*, 43(7):1203 – 1216, 2001.
- [33] G. Grundmeier, W. Schmidt, and M. Stratmann. Corrosion protection by organic coatings: electrochemical mechanism and novel methods of investigation. *Electrochimica Acta*, 45(1516):2515 – 2533, 2000.
- [34] Jilin Yu, Erheng Wang, Jianrong Li, and Zhijun Zheng. Static and low-velocity impact behavior of sandwich beams with closed-cell aluminum-foam core in three-point bending. *International Journal of Impact Engineering*, 35(8):885 – 894, 2008. Twenty-fifth Anniversary Celebratory Issue Honouring Professor Norman Jones on his 70th Birthday.



- [35] Michael Dornbusch. The use of modern electrochemical methods in the development of corrosion protective coatings. *Progress in Organic Coatings*, 61(24):240 – 244, 2008. [Coatings Science International 2007](#).
- [36] L. Matos Filipe, Telmo G. Santos, S. Valtchev, J. Pamies Teixeira, and R.M. Miranda. New method employing the electrical impedance for monitoring mechanical damage evolution in glass-reinforced: Applications to riveted joints. *Materials & Design*, 42(0):25 – 31, 2012.
- [37] Y Sugimura, J Meyer, MY He, H Bart-Smith, J Grenstedt, and AG Evans. On the mechanical performance of closed cell al alloy foams. *Acta materialia*, 45(12):5245–5259, 1997.
- [38] Tetsuji Miyoshi, Masao Itoh, Shigeru Akiyama, and Akira Kitahara. Alporas aluminum foam: production process, properties, and applications. *Advanced engineering materials*, 2(4):179–183, 2000.
- [39] Yongliang Mu, Guangchun Yao, Lisi Liang, Hongjie Luo, and Guoyin Zu. Deformation mechanisms of closed-cell aluminum foam in compression. *Scripta Materialia*, 63(6):629 – 632, 2010.
- [40] Yongliang Mu, Guangchun Yao, and Hongjie Luo. Effect of cell shape anisotropy on the compressive behavior of closed-cell aluminum foams. *Materials & Design*, 31(3):1567 – 1569, 2010.
- [41] H Bart-Smith, A.-F Bastawros, D.R Mumm, A.G Evans, D.J Sypeck, and H.N.G Wadley. Compressive deformation and yielding mechanisms in cellular al alloys determined using x-ray tomography and surface strain mapping. *Acta Materialia*, 46(10):3583 – 3592, 1998.
- [42] H Bart-Smith, JW Hutchinson, and AG Evans. Measurement and analysis of the structural performance of cellular metal sandwich construction. *International journal of mechanical sciences*, 43(8):1945–1963, 2001.
- [43] Y Sugimura, A Rabiei, A.G Evans, A.M Harte, and N.A Fleck. Compression fatigue of a cellular al alloy. *Materials Science and Engineering: A*, 269(12):38 – 48, 1999.
- [44] Lorna J Gibson and Michael F Ashby. *Cellular solids: structure and properties*. Cambridge university press, 1999.
- [45] OB Olurin, Norman A Fleck, and Michael F Ashby. Deformation and fracture of aluminium foams. *Materials Science and Engineering: A*, 291(1):136–146, 2000.

- [46] K.Y.G McCullough, N.A Fleck, and M.F Ashby. Toughness of aluminium alloy foams. *Acta Materialia*, 47(8):2331 – 2343, 1999.
- [47] A.-M. Harte, N.A. Fleck, and M.F. Ashby. Fatigue failure of an open cell and a closed cell aluminium alloy foam. *Acta Materialia*, 47(8):2511 – 2524, 1999.
- [48] O.B. Olurin, K.Y.G. McCullough, N.A. Fleck, and M.F. Ashby. Fatigue crack propagation in aluminium alloy foams. *International Journal of Fatigue*, 23(5):375 – 382, 2001.
- [49] K.Y.G. McCullough, N.A. Fleck, and M.F. Ashby. Uniaxial stress strain behaviour of aluminium alloy foams. *Acta Materialia*, 47(8):2323 – 2330, 1999.
- [50] V.S. Deshpande and N.A. Fleck. Isotropic constitutive models for metallic foams. *Journal of the Mechanics and Physics of Solids*, 48(67):1253 – 1283, 2000.
- [51] J.B. Sha and T.H. Yip. In situ surface displacement analysis on sandwich and multilayer beams composed of aluminum foam core and metallic face sheets under bending loading. *Materials Science and Engineering: A*, 386(12):91 – 103, 2004.
- [52] A.E. Simone and L.J. Gibson. Effects of solid distribution on the stiffness and strength of metallic foams. *Acta Materialia*, 46(6):2139 – 2150, 1998.
- [53] H. Bart-Smith, J.W. Hutchinson, and A.G. Evans. Measurement and analysis of the structural performance of cellular metal sandwich construction. *International Journal of Mechanical Sciences*, 43(8):1945 – 1963, 2001.
- [54] O Kesler and L.J Gibson. Size effects in metallic foam core sandwich beams. *Materials Science and Engineering: A*, 326(2):228 – 234, 2002.
- [55] TM McCormack, R Miller, O Kesler, and LJ Gibson. Failure of sandwich beams with metallic foam cores. *International Journal of Solids and Structures*, 38(28):4901–4920, 2001.
- [56] H. Bart-Smith, J.W. Hutchinson, N.A. Fleck, and A.G. Evans. Influence of imperfections on the performance of metal foam core sandwich panels. *International Journal of Solids and Structures*, 39(19):4999 – 5012, 2002.

- [57] C Chen, AM Harte, and NA Fleck. The plastic collapse of sandwich beams with a metallic foam core. *International Journal of Mechanical Sciences*, 43(6):1483–1506, 2001.
- [58] Craig A. Steeves and Norman A. Fleck. Material selection in sandwich beam construction. *Scripta Materialia*, 50(10):1335 – 1339, 2004.
- [59] J.L. Yu, X Wang, Z.G Wei, and E.H Wang. Deformation and failure mechanism of dynamically loaded sandwich beams with aluminum-foam core. *International Journal of Impact Engineering*, 28(3):331 – 347, 2003. *Fourth International Symposium on Impact Engineering*.
- [60] Maizlinda I Idris, T Vondenitcharova, and M Hoffman. Contact damage response of carbon fibre skin/closed-cell aluminum foam sandwich composites. In *16th International Conference on Composite Materials*, 2007.
- [61] S. Payan, Y. Le Petitcorps, J.-M. Olive, and H. Saadaoui. Experimental procedure to analyse the corrosion mechanisms at the carbon/aluminium interface in composite materials. *Composites Part A: Applied Science and Manufacturing*, 32(3 4):585 – 589, 2001.
- [62] F Bellucci. Galvanic corrosion between nonmetallic composites and metals ii. effect of area ratio and environmental degradation. *Corrosion*, 48(4):281–291, 1992.
- [63] Mohammadreza Tavakkolizadeh and Hamid Saadatmanesh. Galvanic corrosion of carbon and steel in aggressive environments. *Journal of Composites for construction*, 5(3):200–210, 2001.
- [64] Robert Ireland, Luciana Arronche, and Valeria La Saponara. Electrochemical investigation of galvanic corrosion between aluminum 7075 and glass fiber/epoxy composites modified with carbon nanotubes. *Composites Part B: Engineering*, 43(2):183–194, 2012.
- [65] <http://www.alspi.com/introduction.htm>.
- [66] ASTM Standard. C393–00. *Standard test method for flexural properties of sandwich constructions*. West Conshohocken (PA): ASTM International, 2000.
- [67] ASTM Standard. D790-03. *Standard Test Methods for Flexural Properties of Unreinforced and Reinforced Plastics and Electrical Insulating Materials*,” ASTM International, West Conshohocken, PA, 2003.

- [68] Alporas - Aluminum Foam Specification sheet.
- [69] T. Prosek, A. Nazarov, U. Bexell, D. Thierry, and J. Serak. Corrosion mechanism of model zincmagnesium alloys in atmospheric conditions. *Corrosion Science*, 50(8):2216 – 2231, 2008.
- [70] Hassan Mahfuz, Muhammad S Islam, Vijaya K Rangari, Mrinal C Saha, and Shaik Jeelani. Response of sandwich composites with nanophased cores under flexural loading. *Composites Part B: Engineering*, 35(6):543–550, 2004.

## ABSTRACT

### MECHANICAL AND ELECTRO-CHEMICAL INVESTIGATION OF CARBON FARBRIC/EPOXY AND ALUMINUM FOAM SANDWICH COMPOSITE BEAMS

by

**NARIN SARA FATIMA**

**April 2013**

**Advisor:** Dr. Golam Newaz

**Major:** Mechanical Engineering

**Degree:** Master of Science

In this study the mechanical and electrochemical response of a sandwich composite comprising of carbon fiber fabric skin and aluminum foam core was evaluated. The three point flexural test was chosen to investigate the mechanical behavior in terms of finding the deformation and failure behavior. The flexural test exhibited an excellent bond between the skin and the core. The specimens mainly failed in three different modes - indentation, core shear and face yielding and showed three distinct regions: a linear rise in load with displacement region, a rapid load drop region and a plateau region followed by a densification region. Due high potential difference between carbon and aluminum, another part of this study was to investigate if this sandwich structure creates a galvanic cell in presence of an electrolyte. For this purpose four point probe electrode measurement method was used to monitor corrosion in the sandwich beam through change in the aluminum cores electrical resistance over. The effectiveness of a insulating barrier layer in preventing galvanic corrosion was also investigated and it was found that a polymer based glass fiber system is ineffective in preventing corrosion in these sandwich structures. The most efficient way to prevent galvanic corrosion in these type of composite beams is by insulating the dissimilar material system from the environment thus not allowing any electrolyte to come in contact.

## AUTOBIOGRAPHICAL STATEMENT

**Name:** NARIN SARA FATIMA

**Place of Birth:** DHAKA, BANGLADESH

### EDUCATION:

- **MASTERS OF SCIENCE in Mechanical Engineering**, at  
Wayne State University, Detroit, Michigan [2011-2013]
- **BACHELOR OF SCIENCE in Mechanical Engineering**, at  
Bangladesh University of Engineering & Technology, Dhaka, Bangladesh [2004-2009]

### EXPERIENCE:

- **GRADUATE RESEARCH ASSISTANT** [2012-2013]  
Advanced Composite Research Laboratory,  
Wayne State University, Detroit, Michigan.
- **STUDENT ASSISTANT** [2011]  
Planning, Facility & Management,  
Wayne State University, Detroit, Michigan.
- **ENGINEER - PRODUCT SUPPORT MARKETING DIVISION** [2010-2011]  
Bangla Trac Ltd. (Exclusive dealer of all CATERPILLAR products in Bangladesh),  
Mohakhali, Dhaka, Bangladesh.